



3 4456 0361022 4

# AEC RESEARCH AND DEVELOPMENT REPORT

ORNL-2128 *Cy-5-A*  
Reactors-Special Features  
of Military Package Power Reactors

## ARMY PACKAGE POWER REACTOR

### CRITICAL EXPERIMENT

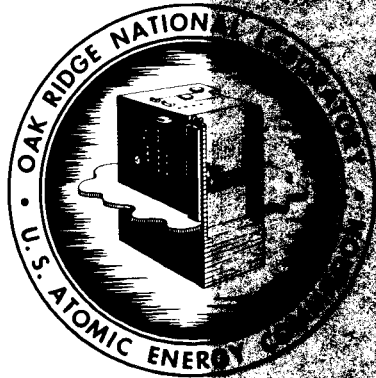
- D. V. P. Williams
- D. W. Magnuson
- M. L. Batch
- W. R. Johnson
- L. K. Leslie
- A. D. Callihan

CEN  
D

**LIB**

DO NOT

If you wish to examine this document  
send in request with document number and we will  
arrange to loan it to you.



## OAK RIDGE NATIONAL LABORATORY

OPERATED BY

### UNION CARBIDE NUCLEAR COMPANY

A Division of Union Carbide and Carbon Corporation



POST OFFICE BOX P • OAK RIDGE, TENNESSEE

LEGAL NOTICE

This report was prepared as an account of Government sponsored work. Neither the United States, nor the Commission, nor any person acting on behalf of the Commission:

- A. Makes any warranty or representation, express or implied, with respect to the accuracy, completeness, or usefulness of the information contained in this report, or that the use of any information, apparatus, method, or process disclosed in this report may not infringe privately owned rights; or
- B. Assumes any liabilities with respect to the use of, or for damages resulting from the use of any information, apparatus, method, or process disclosed in this report.

As used in the above, "person acting on behalf of the Commission" includes any employee or contractor of the Commission to the extent that such employee or contractor prepares, handles or distributes, or provides access to, any information pursuant to his employment or contract with the Commission.

ORNL 2128

This document consists of 84 pages

Copy 5 of 179 copies. Series A

Contract No. W-7405-eng-26

Applied Nuclear Physics Division

ARMY PACKAGE POWER REACTOR CRITICAL EXPERIMENT

D. V. P. Williams  
D. W. Magnuson  
M. L. Batch, Babcock and Wilcox  
W. R. Johnson, Alco Products, Inc.  
J. K. Leslie, Alco Products, Inc.  
Dixon Callihan

Date Issued

AUG 8 1956

**DECLASSIFIED**

CLASSIFICATION CHANGED TO:

BY AUTHORITY OF: T10-1151

BY: D. Morrison 6/26/57

OAK RIDGE NATIONAL LABORATORY

Operated by

UNION CARBIDE NUCLEAR COMPANY

A Division of Union Carbide and Carbon Corporation

Post Office Box P

Oak Ridge, Tennessee

[REDACTED]

[REDACTED]



3 4456 0361022 4

Reactors-Special Features of  
Military Package Power Reactors  
M-3679 (18th ed.)

INTERNAL DISTRIBUTION

- |                                     |                                   |
|-------------------------------------|-----------------------------------|
| 1. C. E. Center                     | 49. A. S. Householder             |
| 2. Biology Library                  | 50. C. P. Keim                    |
| 3. Health Physics Library           | 51. C. S. Harrill                 |
| 4-5. Central Research Library       | 52. C. E. Winters                 |
| 6. Reactor Experimental             | 53. D. S. Billington              |
| 7. Engineering Library              | 54. D. W. Cardwell                |
| 7-26. Laboratory Records Department | 55. E. M. King                    |
| 27. Laboratory Records, ORNL R.C.   | 56. A. J. Miller                  |
| 28. A. M. Weinberg                  | 57. E. P. Blizard                 |
| 29. L. B. Loeb (K-25)               | 58. D. D. Cowen                   |
| 30. J. P. Murray (Y-12)             | 59. W. M. Breazeale (consultant)  |
| 31. J. A. Swannout                  | 60. M. J. Skinner                 |
| 32. E. H. Taylor                    | 61. R. B. Murray                  |
| 33. E. D. Shipley                   | 62. R. R. Dickison                |
| 34. A. H. Snell                     | 63. A. Simon                      |
| 35. M. L. Nelson                    | 64. F. C. Maienschein             |
| 36. W. H. Jordan                    | 65. R. R. Bate                    |
| 37. S. J. Cromer                    | 66. H. G. Blosser                 |
| 38. G. E. Boyd                      | 67. A. L. Boch                    |
| 39. R. A. Charpie                   | 68. A. D. Callihan                |
| 40. S. C. Lind                      | 69. C. E. Clifford                |
| 41. F. L. Culler                    | 70. J. E. Cunningham              |
| 42. A. Hollaender                   | 71. W. K. Ergen                   |
| 43. J. H. Frye, Jr.                 | 72. E. E. Gross                   |
| 44. M. T. Kelley                    | 73. R. Gwin                       |
| 45. G. H. Clewett                   | 74. D. W. Magnuson                |
| 46. R. S. Livingston                | 75. F. H. Neill                   |
| 47. K. Z. Morgan                    | 76. A. M. Perry                   |
| 48. T. A. Lincoln                   | 77. L. D. Schaffer                |
|                                     | 78. ORNL - Y-12 Technical Library |

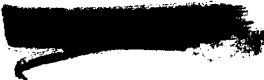
EXTERNAL DISTRIBUTION

- 79. Division of Research and Development, EC, ORO
- 80-179. Given distribution as shown in M-3679 for Reactors-Special Features of Military Package Power Reactors category



ACKNOWLEDGEMENTS

The Army Package Power Reactor Critical Experiments involved the cooperative efforts of several groups; notably the Package Power Reactor Group of the Electronuclear Research Division, the Metallurgy Division and the Atomic Energy Department of Alco Products, Inc. A. M. Perry, R. R. Bate and J. G. Gallagher assisted in the conceptual design. The equipment design was detailed by J. E. Mann and H. G. Blosser, who, with J. H. Cupp, supervised the construction and assembly. Control rods, boron plates, and special APPR-type elements were fabricated by the ORNL Metallurgy Division, under the direction of R. J. Beaver and R. C. Waugh. H. G. Blosser assisted in the planning and performance of several of the experiments. While the experimental program was in progress, the need for additional nuclear data for the reactor design became apparent, and many of the experiments in the program were added at the request and suggestion of J. L. Meem and J. G. Gallagher of Alco Products, Inc.

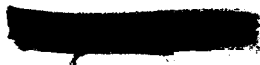
  
Table of Contents

	Pg. No.
ABSTRACT . . . . .	1
INTRODUCTION . . . . .	2
I. DESCRIPTION OF EQUIPMENT . . . . .	2
II. CRITICAL MASS EVALUATIONS . . . . .	12
Cold Clean Critical Mass . . . . .	12
Critical Mass with Boron Poisoning . . . . .	14
III. FUEL EVALUATION . . . . .	14
Radial Fuel Importance . . . . .	17
Determination of the Specific Mass Reactivity Coefficient . . . . .	18
IV. EFFECTS OF HETEROGENEITY ON CRITICAL MASS . . . . .	20
Homogeneous Element . . . . .	20
APPR-Type Element . . . . .	22
Analysis of Heterogeneity Effects . . . . .	23
V. APPR CONTROL ROD EVALUATION . . . . .	26
Rod Measurements with Clean Core . . . . .	26
Calibration of Eccentric Rod No. 37 . . . . .	29
Rod Measurements with Boron-Poisoned Core . . . . .	29
Mockup of the APPR-1 Control Rods . . . . .	32
VI. NEUTRON FLUX AND POWER DISTRIBUTION MEASUREMENTS . . . . .	32
Description of Detectors . . . . .	32
Results . . . . .	33
APP. A. DETAILED COMPONENT SPECIFICATIONS . . . . .	67
APP. B. SPECTROGRAPHIC ANALYSIS OF TYPE 304 STAINLESS STEEL . . . . .	70
APP. C. FUEL PLATE FABRICATION . . . . .	72
APP. D. TYPICAL PLATE ARRANGEMENTS WITHIN A FUEL ELEMENT . . . . .	74
APP. E. CALCULATION OF METAL VOLUME PERCENT IN CORE . . . . .	75

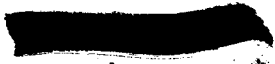
[REDACTED]

LIST OF TABLES

	Pg. No.
1. Clean Critical Mass as a Function of the Metal Volume Percent . . . . .	12
2. Critical Mass as a Function of Void Volume of Fuel Plates . . .	14
3. Critical Mass as a Function of Boron Loading . . . . .	17
4. Radial Fuel Evaluation . . . . .	18
5. Specific Mass Reactivity Coefficient for Several Critical Loadings . . . . .	20
6. Reactivity Changes Effected by Homogeneous Element Substitutions . . . . .	22
7. Reactivity Changes Effected by APPR-Type Element Substitutions . . . . .	23
8. Critical Mass of Cores Consisting of Special Elements . . . . .	24
9. Mass and Reactivity Values of Various Rod Configurations in the Clean Core . . . . .	27
10. Rod Interactions . . . . .	29
11. APPR Rod No. 37 Calibration . . . . .	30
12. Mass Values of Various Rod Configurations in the Boron Poisoned Core . . . . .	30
13. Reactor Loading for the Mockup of Seven APPR-1 Control Rods . .	32
14. Summary of Neutron Flux and Power Distribution Measurements . .	34
15. Horizontal Flux Distribution in Clean Reactor . . . . .	35
16. Horizontal Flux Distribution in Reactor Containing 255 g of Boron . . . . .	37
17. Horizontal Flux Distribution in Clean Reactor with Central APPR Rod Inserted . . . . .	37
18. Vertical Flux Distribution in Element 23 of Clean Reactor . . .	40
19. Vertical Flux Distribution in Element 30 of Clean Reactor with Central APPR Rod Inserted . . . . .	43
20. Horizontal Power Distribution at Midplane in Clean Reactor . .	43



	Pg. No.
21. Horizontal Power Distribution in Reactor Containing 255 g of Boron . . . . .	47
22. Diagonal Power Distribution in Reactor Containing 255 g of Boron . . . . .	47
23. Horizontal Power Distribution in Clean Reactor with Central APPR Rod Inserted . . . . .	47
24. Horizontal Power Distribution in Clean Reactor with Five APPR Rods Half Inserted . . . . .	51
25. Vertical Power Distribution in Clean Reactor . . . . .	51
26. Vertical Power Distribution in Element 23 of Reactor Containing 255 g of Boron . . . . .	54
27. Vertical Power Distribution in Clean Reactor with Five APPR Rods Half Inserted . . . . .	54
28. Microscopic Flux Traverse in Clean Reactor, Perpendicular to Fuel . . . . .	57
29. Microscopic Flux Traverse in Clean Reactor with APPR Element in Position 23 . . . . .	59
30. Microscopic Flux Traverse in Clean Reactor Parallel to Fuel . . . . .	59
31. Microscopic Flux Traverse in Reactor Containing 255 g of Boron . . . . .	62
32. Flux Distribution at Perimeter of Element 23 in Reactor Containing 255 g of Boron . . . . .	62
33. Power Distributions at Corner of Clean Reactor . . . . .	65



[REDACTED]

LIST OF FIGURES

	Pg. No.
1. The APPR Critical Experiment . . . . .	4
2. Fuel Box Partially Loaded with Fuel and Stainless Steel Plates . . . . .	5
3. Top View of the APPR Critical Experiment . . . . .	6
4. Components of the APPR Critical Experiment . . . . .	7
5. APPR Fuel Box Schematic . . . . .	8
6. APPR Critical Assembly Schematic . . . . .	11
7. Clean Critical Mass as a Function of the Metal Volume Percent . .	13
8. Critical Mass as a Function of Void Volume of Fuel Plates . . . .	15
9. Critical Mass as a Function of Boron Loading . . . . .	16
10. Radial Fuel Evaluation . . . . .	19
11. Specific Mass Reactivity Coefficient for Several Critical Loadings . . . . .	21
12. Calculated Critical Mass of APPR as a Function of Boron Loading .	25
13. Calibration of Five Ganged APPR Control Rods . . . . .	28
14. APPR Rod No. 37 Calibration . . . . .	31
15. Horizontal Flux Distribution in Clean Reactor . . . . .	36
16. Horizontal Flux Distribution in Reactor Containing 255 g of Boron . . . . .	38
17. Horizontal Flux Distribution in Clean Reactor with Central APPR Rod Inserted . . . . .	39
18. Vertical Flux Distribution in Element 23 of Clean Reactor Without End Boxes . . . . .	41
19. Vertical Flux Distribution in Element 23 of Clean Reactor With End Boxes . . . . .	42
20. Vertical Flux Distribution in Element 30 of Clean Reactor with the Central APPR Rod Inserted . . . . .	44

	Pg. No.
21. Horizontal Power Distribution at Midplane in Clean Reactor, Perpendicular to Fuel . . . . .	45
22. Horizontal Power Distribution at Midplane in Clean Reactor, Parallel to Fuel . . . . .	46
23. Horizontal Power Distribution in Reactor Containing 255 g of Boron . . . . .	48
24. Diagonal Power Distribution in Reactor Containing 255 g of Boron . . . . .	49
25. Horizontal Power Distribution in Clean Reactor with Central APPR Rod Inserted . . . . .	50
26. Horizontal Power Distribution in Clean Reactor with Five APPR Rods Half Inserted . . . . .	52
27. Vertical Power Distribution in Clean Reactor.	53
28. Vertical Power Distribution in Element 23 of Reactor Containing 255 g of Boron . . . . .	55
29. Vertical Power Distribution in Clean Reactor with Five APPR Rods Half Inserted . . . . .	56
30. Microscopic Flux Traverse in Clean Reactor, Perpendicular to Fuel . . . . .	58
31. Microscopic Flux Traverse in Clean Reactor with APPR Element in Position 23 . . . . .	60
32. Microscopic Flux Traverse in Clean Reactor Parallel to Fuel . .	61
33. Microscopic Flux Traverse in Reactor Containing 255 g of Boron . . . . .	63
34. Flux Distribution at Perimeter of Element 23 in Reactor Containing 255 g of Boron . . . . .	64
35. Power Distributions at Corner of Clean Reactor . . . . .	66

[REDACTED]

ABSTRACT

A zero power mockup of the Army Package Power Reactor was constructed in the Oak Ridge National Laboratory Critical Experiment Facility. The assembly consisted of 45 fuel elements, in a 7 x 7 array with the corners removed, and was contained in a large water tank. The over-all core dimensions were 21 x 21 x 22 in. Enriched uranium metal foils, 2.5 x 0.002 x 22.0 in., each containing 31.1 g of U-235, were encased in stainless steel sheets to form the fuel plates. Additional plates of stainless steel and of boron encased in stainless steel were used to simulate materials of the APPR-1 core. Each type of plate contained essentially the same amount of steel. When the 18 slots of each element were loaded with plates, the metal volume fraction was 0.197 and was kept constant throughout the experimental program. The number of fuel plates per element varied from 7.5 for the clean reactor to 14.5 for a boron-poisoned assembly. The critical mass of the clean reactor was  $10.35 \pm 0.05$  kg of U-235. The addition of 255 g of natural boron to the core, distributed among three plates in each element, increased the critical mass to 20.1 kg of U-235.

Reactivity coefficients of fuel plates, measured in the clean reactor as a function of position, gave an average fuel value of 0.526¢/g. The specific mass reactivity coefficient,  $m\Delta k/k\Delta m$ , was determined over a wide range of reactor loadings.

The effects of the heterogeneous distributions of the uranium and boron on the critical masses of the reactor were studied by exchanging special fuel elements with assembly elements in several locations and noting the resulting changes in reactivity. These data and the assumption that the specific mass reactivity coefficient is constant for small changes in fuel loading were used to calculate a value of 9.1 kg of U-235 for the critical mass of an unpoisoned array of APPR-type elements.

Measurements were made of the value of the APPR control rods in various locations, both individually and collectively, in terms of the additional mass of U-235 necessary to maintain criticality. One eccentric control rod fully inserted was worth 0.68 kg of U-235, the central control rod 1.70 kg, and five rods fully inserted required an addition of 12.23 kg to the loading. In addition, the calibration of one eccentric rod by incremental periods gave a value of \$3.8.

Power and neutron flux distribution measurements were made in all major configurations of the critical assembly. Macroscopic neutron flux distributions were measured by exposing bare and cadmium-covered gold foils at various points in the reactor. Intercell flux distributions were obtained using dysprosium as the neutron detector. The power distributions were found by measuring the fission fragment activity on aluminum catcher foils placed in contact with the uranium in special fuel plates. Catcher foils, exposed both bare and cadmium-covered, in the midplane of the clean reactor, indicated that 91% of the fissions were produced by neutrons having energies less than about 0.5 ev.

## INTRODUCTION

Early in 1953 the Oak Ridge National Laboratory was requested by the Army Reactor Branch of the AEC to survey the reactor field and propose a design for a small nuclear power plant to be installed in remote or relatively inaccessible locations. As a result of this survey a pressurized-water, package, power reactor was designed,<sup>1</sup> and critical experiments were planned in support of this design. A contract, awarded to Alco Products, Incorporated, to build a prototype package reactor, Army Package Power Reactor-1 (APPR-1), at Fort Belvoir, Virginia, included an agreement for certain critical experiments to be performed at ORNL.

The results of critical experiments for the Army Package Power Reactor are herein recorded, including measurements of critical mass, flux and power distributions, and an evaluation of design control rods. The primary effort was to obtain necessary engineering data for APPR-1. No attempt has been made to analyze the results further than that required to report the data meaningfully. These data have been applied to the reactor design, and reference is made<sup>2,3</sup> to these reports for a detailed interpretation of the results.

### I. DESCRIPTION OF EQUIPMENT

The APPR critical assembly<sup>4,5,6,7</sup> was designed to mock up as nearly as possible the actual APPR core as described by Boch *et al.*<sup>1</sup> The assembly consisted of 45 fuel boxes arranged as a 7 x 7 array with the four corners removed. Fuel boxes were held in place by grid structures at the top and bottom, and a stainless steel skirt or side wall defined the outer perimeter of the core. A rectangular frame supported the assembly and also provided the support structure for control and safety rod drive mechanisms above the core. The entire system was contained in a large water tank which was filled during normal operation to provide a neutron moderator and an effective infinite neutron reflector on all sides of the active core.

- 
1. A. L. Boch, W. R. Gall, G. F. Leichsenring, and R. S. Livingston, "A Conceptual Design of a Pressurized-Water Package Power Reactor", ORNL-1613 Revised (Nov. 1955).
  2. R. L. Murray *et al.*, "Nuclear Calculations and Analyses of Critical Experiments for the Army Package Power Reactor," ORNL-2075 (To be published).
  3. J. G. Gallagher *et al.*, "Reactor Analysis for the APPR-1," AP&E-7.
  4. J. G. Gallagher *et al.*, "APPR Critical Experiment," ORNL-CF-55-5-112 (May 18, 1955).
  5. J. G. Gallagher and R. R. Bate, "Boron Plate Specifications for APPR Critical Experiment," ORNL-CF-55-5-32 (May 4, 1955).
  6. H. G. Blosser, "Control Rod Absorber Section Specifications for Critical Experiment," ORNL-CF-55-6-165, (June 28, 1955).
  7. J. G. Gallagher, H. G. Blosser and J. E. Mann, "Test Element for APPR Critical Experiment," ORNL-CF-55-11-66 (Nov. 9, 1955).

Figure 1 is a photograph of the APPR critical experiment, and various components of the assembly are illustrated in Figs. 2, 3, and 4. Detailed component specifications are given in Appendix A.

The fuel boxes<sup>4</sup> were made of type 304 stainless steel plate, the over-all box dimensions being 2.81 x 2.85 x 31 in. The two opposite sides of each box contained 18 grooves, 0.050 x 0.056 in., forming slots into which either fuel, steel, or boron plates could be positioned (see Figs. 2, 3, and 5).

Cylinders of stainless steel which were designed to give the same metal-to-water ratio as the end boxes of the fuel elements in the top and bottom reflector were fitted into each fuel box. Figure 4 is a photograph which includes these stainless steel cylinders. Some are shown in place in the assembly in Figs. 1 and 3. The perimeter skirt of stainless steel was 0.056 in. thick.

Materials were added to the core of the assembly in the form of plates and because of the necessity for flexibility, plates were made of each individual material. All plates were designed so that the metal volume percent (about 20%) in the core would remain constant, if all 18 slots were filled, no matter what changes were made in the amounts of uranium and boron. The slotted sides of the fuel box held the plates in position.

Fuel plates<sup>4</sup> consisted of an enriched (93.2%) uranium foil, 2.50 x 0.002 x 22.0 in., encased in type 304 stainless steel sheets, nominally 0.0111 in. thick. To make the fuel plate watertight, the edges of the bottom steel sheet were folded over the top piece, completely enclosing the foil, which in turn was glued to both steel sheets. The over-all dimensions of the fuel plate were 2.723 x 0.025 x 23.0 in. A picture of a fuel plate is included in Fig. 4. Fuel plates were also available with one-half width uranium foils, 1.25 x 0.002 x 22.0 in., for making smaller changes in the uranium loading. These plates had the same dimensions and steel content as the 2.5 in. wide foil plates. Details of the fuel plate fabrication are given in Appendix C.

Since the APPR will contain boron as a burnable poison, boron plates<sup>4,5</sup> were fabricated by putting B<sub>4</sub>C in a sintered iron matrix which was clad with type 304 stainless steel. The clad-core-clad thicknesses were 0.005, 0.015, and 0.005 in., respectively, and the outside dimensions were 2.723 x 0.025 x 23.0 in. Two sets of plates were made, one set containing 1.889 g of natural boron per plate, the other 0.944 g of boron per plate.

The steel plates were made of type 304 stainless steel, the over-all dimensions being 2.723 x 0.025 x 23.0 in. (see Fig. 4). Spectrographic analyses of the steels used in various plates are given in Appendix B.

PHOTO 24922

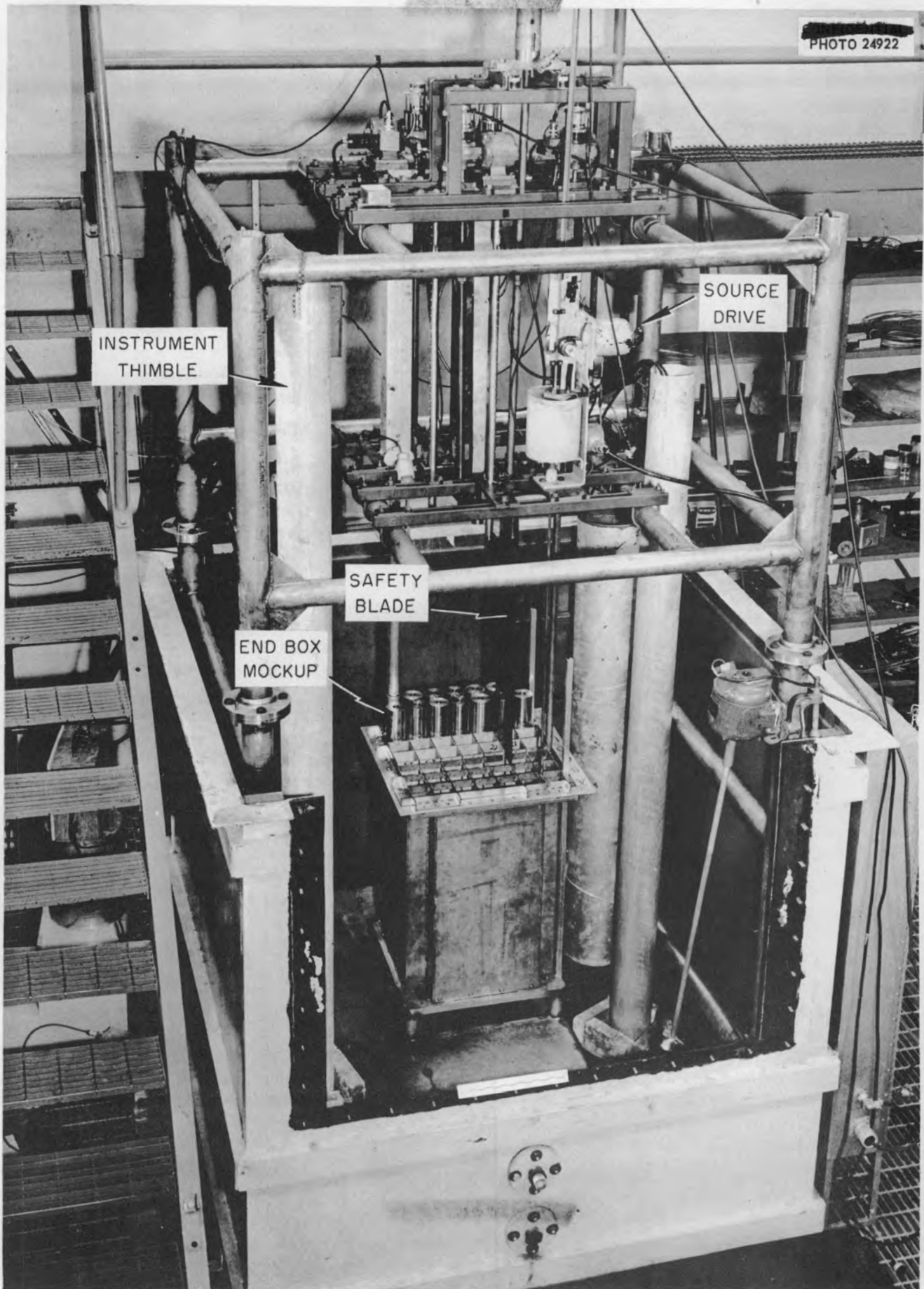


Fig. 1. The APPR Critical Experiment.

PHOTO 24920

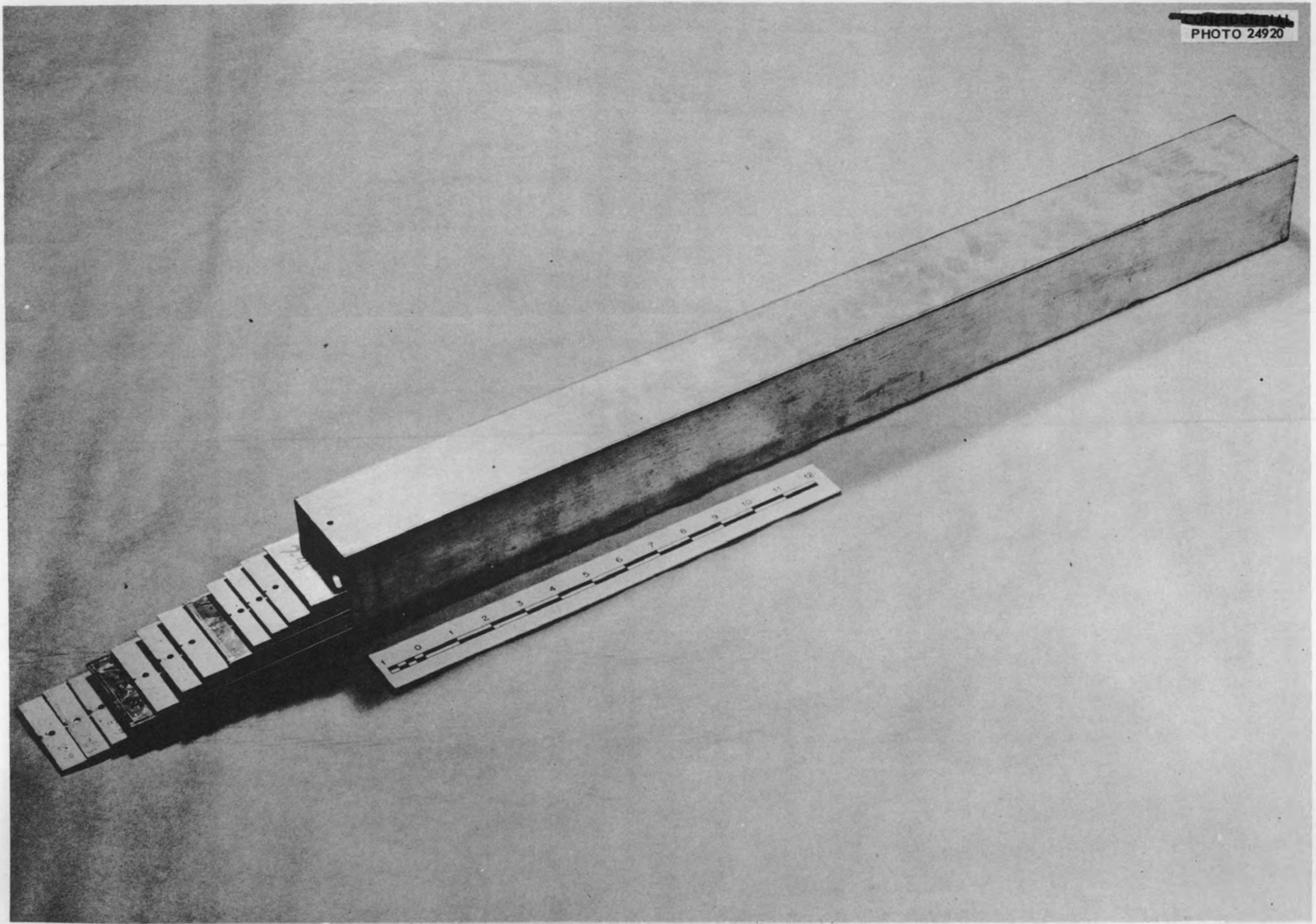


Fig. 2. Fuel Box Partially Loaded with Fuel and Stainless Steel Plates.

PHOTO 24680

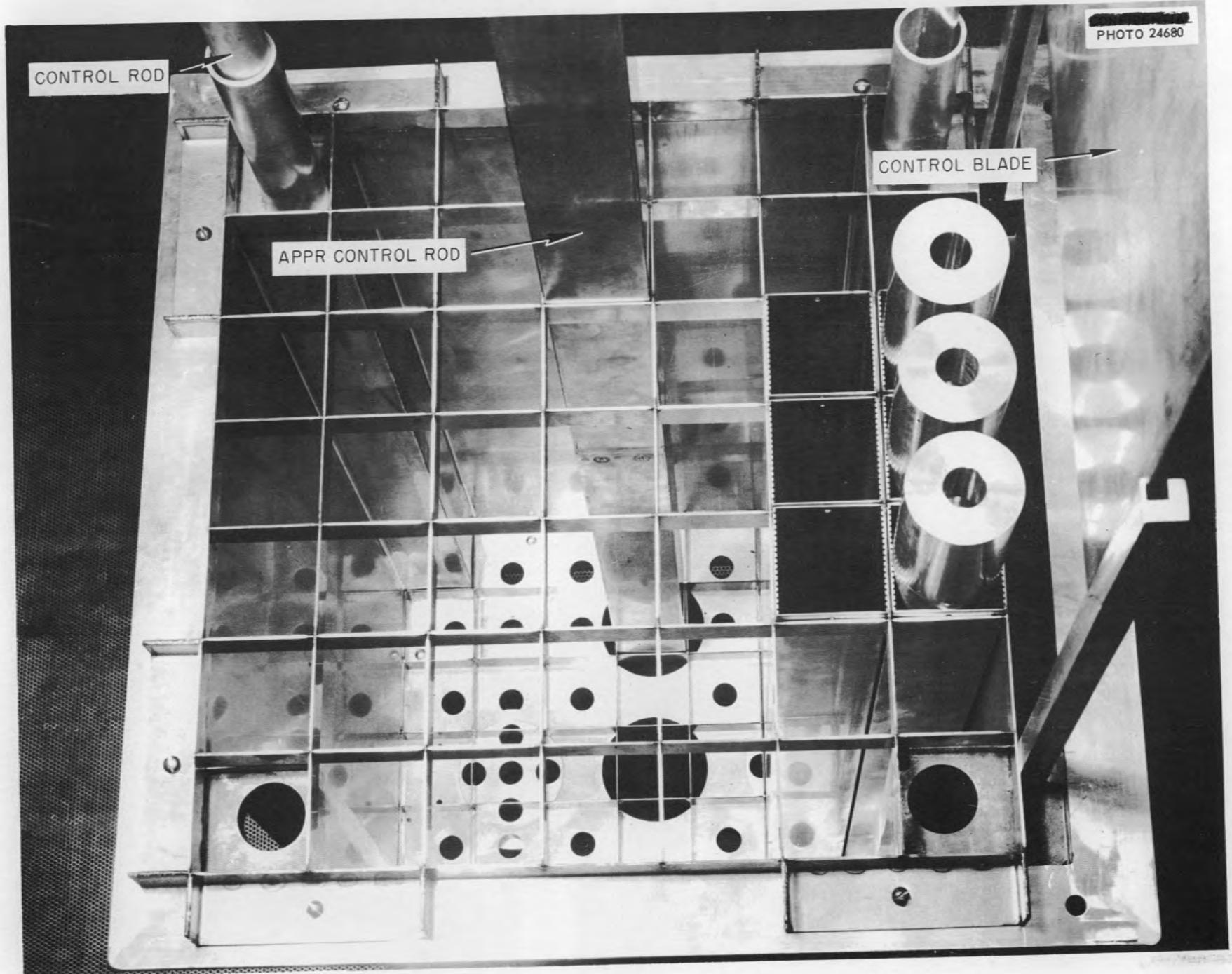


Fig. 3. Top View of the APPR Critical Experiment.

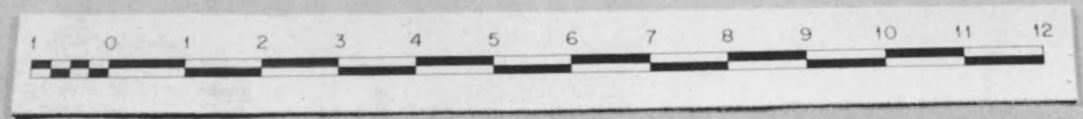
PHOTO 24921

TOP END BOX MOCKUP

BOTTOM END BOX MOCKUP

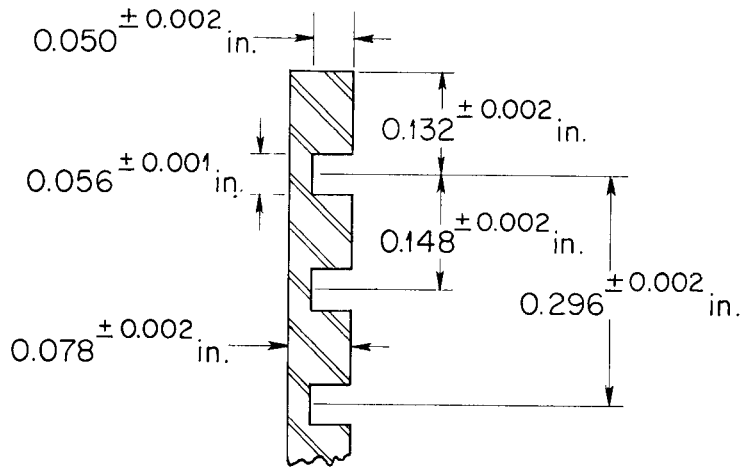
STEEL PLATE

FUEL PLATE



-7-

Fig. 4. Components of the APPR Critical Experiment.



SLOT DETAIL : FUEL BOX

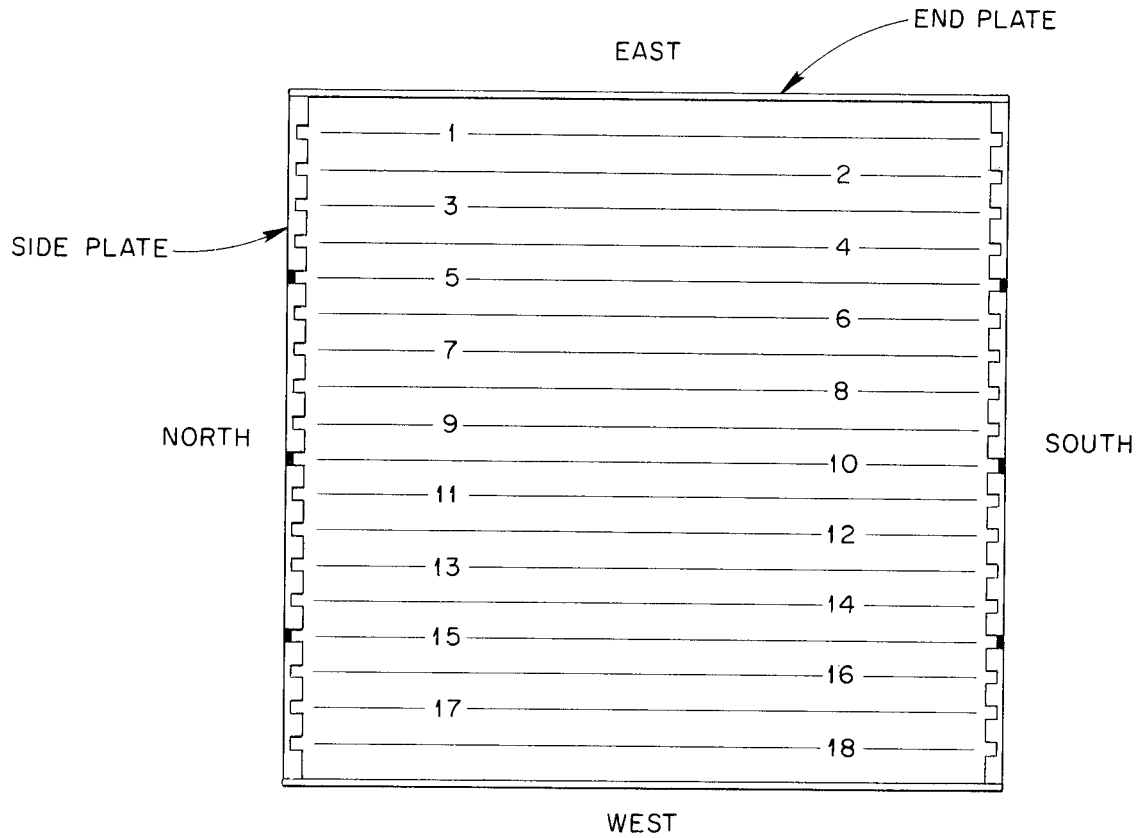


Fig. 5. APPR Fuel Box Schematic.

Control rods consisting of an absorber section and a fuel section, similar to those designed for the APPR, were constructed for these experiments. The absorber section<sup>6</sup> of the experimental rods was a hollow square box, 2.80 x 2.85 x 23.25 in. Each side of the box contained 75 g of boron or 230 mg B/cm<sup>2</sup> in a copper matrix, 2.31 x 22.0 x 0.125 in., clad with 0.036 in. stainless steel. Water filled the center of the absorber section as it was inserted into the core. A removable fuel section, essentially the same as a normal fuel box, was attached to the bottom of each absorber section, and the top of the fuel was 2 in. below the poison in the top section. Holes were left in the bottom supporting structure of the core beneath each of the five control rod positions to allow the fuel section of the rod to protrude below the core as the rod was inserted. Figure 3 shows an APPR rod with the fuel section in the assembly.

Two cadmium blades were used for operational control and safety in the APPR critical experiments. The motor-driven control blade, which was 14 in. wide, was located about 1/2 in. outside of one face of the core and is shown fully withdrawn in Fig. 3. The second cadmium blade was less than 9 in. wide and was positioned above the core so that it would drop between the fuel boxes as a safety mechanism. The safety blade is shown withdrawn in Fig. 1. Both blades were dropped in the event of a scram. In addition to the blades, there was a small control rod in one corner of the core. The positions of these operational controls are shown in Fig. 6. The total reactivity values of the safety and control blades were found using the rod drop method. These experiments indicated that the safety blade was worth  $\beta$ 2, and the control blade value was 30¢. The total value of the control blade, which was found by summation of incremental periods, was 26.5¢, and this was believed to be more accurate.

The polonium-beryllium neutron source, with a strength of approximately  $1.5 \times 10^7$  neutrons/sec, was mounted at the horizontal midplane in a corner of the assembly as shown in Fig. 6. When criticality was achieved, the source was withdrawn into a paraffin cylinder above the assembly. The source drive, paraffin cylinder, and guide tube are discernible in Fig. 1.

Certain terminology and numbering conventions, which have been adopted for denoting particular components of the assembly and for designating positions in the core, are used throughout this report. The various terms and corresponding definitions are as follows:

- |                  |  |
|------------------|--|
| Box or Fuel Box: | One of the stainless steel boxes into which core materials in the form of plates were added. A total of 45 boxes made up the assembly.                               |
| Plate:           | Fuel plates, boron plates, or steel plates which contained uranium and steel, boron and steel, or steel, respectively. A plate is referred to as full or half plate, |

depending on the relative quantity of fuel or boron which the plate contained.

Element or Fuel Element: The box and its plate loading considered as a single component.

Slot: A set of opposite grooves in the sides of a box into which the plates were positioned.

APPR Control Rod: The experimental mockup of the design APPR control rod, consisting of an absorber section and a fuel box which is appropriately loaded and attached to the bottom of the absorber section.

Figures 5 and 6 show the numbering conventions used to locate positions in the core of the assembly. Each of the 45 possible box positions is numbered. A plate in the core may be designated as being in one of the 18 slots of a certain box. Vertical location is given directly as the distance from the top, center or bottom of the core. Examples of these are as follows:

1. An APPR control rod was inserted into position (or box) 23.
2. Foil A was on a fuel plate in box 37, slot 6, on the side facing slot 5, 8 in. from the top of the core.

Conventional instrumentation was employed for safety circuits and operational indication of core power level. During the initial approach to criticality five boron-lined proportional counters were used to measure the subcritical neutron source multiplication. For day-to-day operation three  $\text{BF}_3$  ionization chambers which were located in the tank in watertight cylindrical thimbles, shown in Fig. 1, were the primary control instruments. One of these chambers was connected to provide an indication of the logarithmic neutron level and the reactor period. The other two  $\text{BF}_3$  chambers were attached to linear neutron level recorders. The  $\text{BF}_3$  chambers and a photomultiplier tube, which measured the gamma-ray activity adjacent to the tank, were all attached to the safety scram circuit. An excessively fast reactor period or an excessive power level would have actuated a scram.

Water height in the assembly was indicated by a sight-glass in the control room connected to the bottom of the tank. The top of the sight-glass was vented to the reactor room to avoid erroneous water height indications due to a pressure differential between the two rooms. Water temperature was measured by a number of thermocouples in the tank and recorded in the control room.

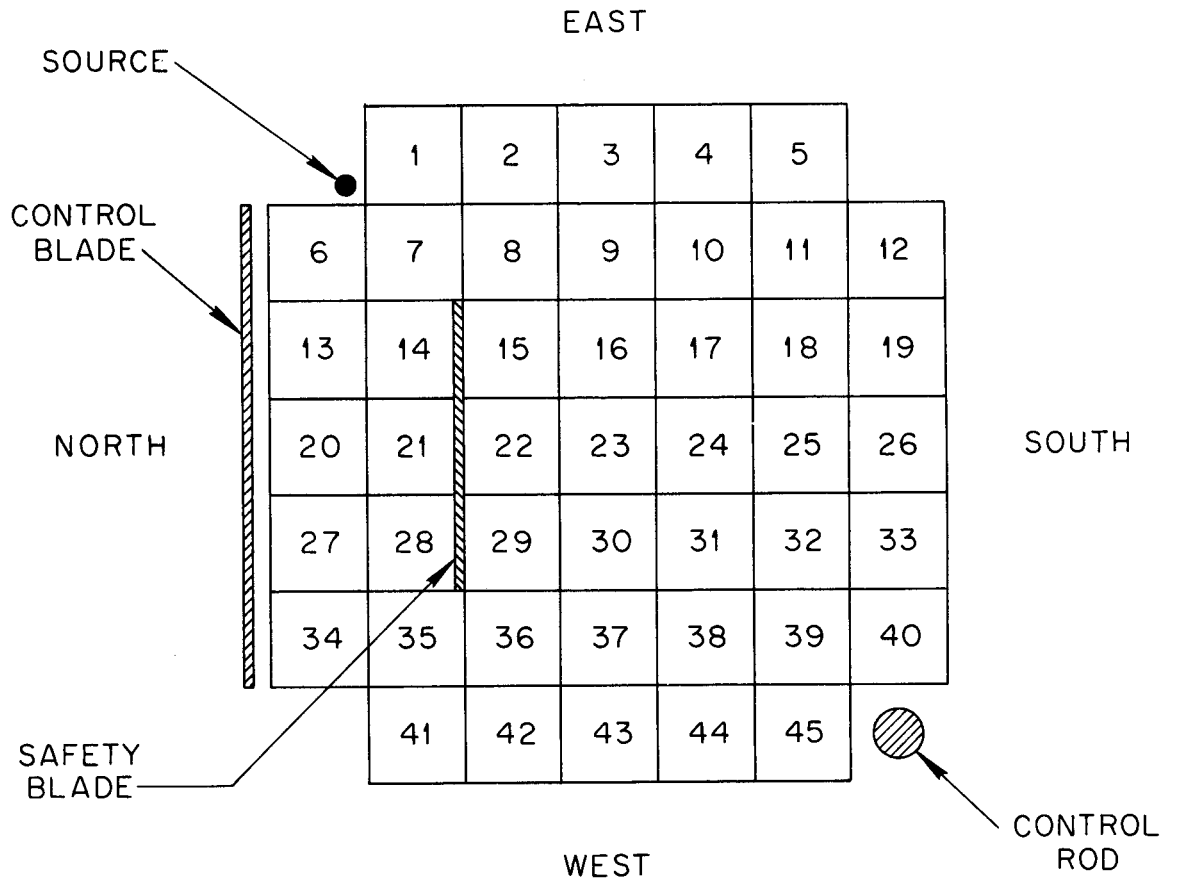


Fig. 6. APPR Critical Assembly Schematic.

II. CRITICAL MASS EVALUATIONS

Cold Clean Critical Mass

The cold, clean critical mass is defined as the mass of fissionable material with which the reactor is critical at room temperature with all rods and poison removed. Several clean critical masses were found for the 7 x 7 array of fuel boxes with corners removed for different metal volume percentages.<sup>8</sup> In addition, the critical masses of two metal volume percentages in a 5 x 5 array were determined. These data are listed in Table 1 for the different arrays, and the dependence of critical mass on metal volume percent is shown in Fig. 7.

Table 1. Critical Masses as a Function of the Metal Volume Percent.

Core Configuration	Metal Content (vol. %)	Critical Mass (kg of U-235)
7 x 7 (corners removed)	19.7	10.5
	18.2	9.9
	9.5	6.6
5 x 5	10.6	4.6
	19.7	7.4

A theoretical equation using empirically determined constants was used to fit critical mass data for cylindrical, aqueous solution, water-reflected reactors of various heights and diameters.<sup>9</sup> This equation was used to predict the critical mass of the cylindrical equivalent of the APPR critical experiment which contains no steel, and this critical mass was 2.7 kg of U-235.<sup>10</sup> An extrapolation of the curve in Fig. 7 to 0% metal volume gives a value of 2.9 kg of U-235. Because of the heterogeneity effects of lumped uranium and steel in the data that define the curve, it is surprising that the extrapolation is found to be in close agreement with the calculated value.

Subsequent to fabrication of the fuel plates, a large fraction of them developed an internal gas pressure, possibly from a uranium-water reaction,

- 
8. See Appendix E for calculations of metal volume percentages for various components of the core.
  9. R. Gwin, "Critical Conditions for Cylindrical, Water-Tamped, and Water-Moderated Reactors," Y-A2-183, (Dec. 2, 1955).
  10. The authors are particularly indebted to R. Gwin for these calculations.

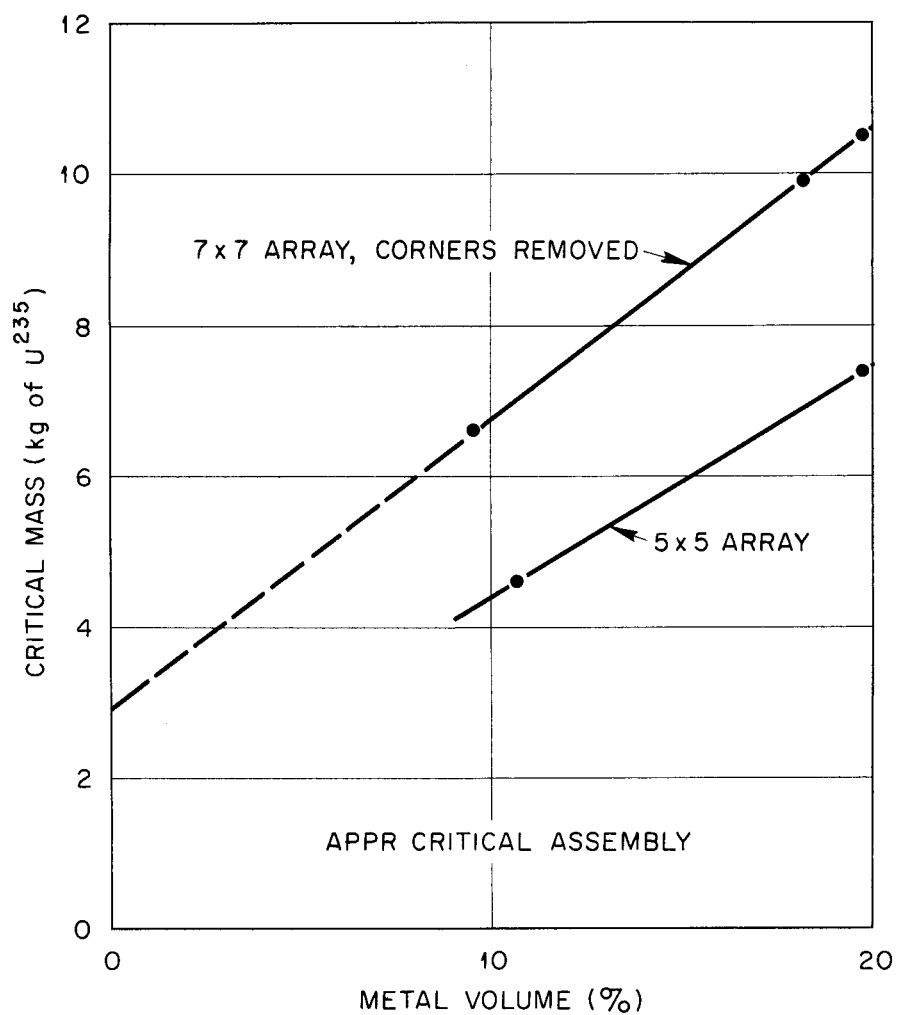


Fig. 7. Clean Critical Mass as a Function of the Metal Volume in Per Cent.

~~CONFIDENTIAL~~

which caused the plates to bulge. This increased volume of the fuel plates displaced water moderator from the assembly and the critical mass was measured as a function of void volume. The volumes of groups of 45 plates were determined by water displacement measurements, and for the reduced volumes observed some of the plates had been opened to vent the accumulated gases. Critical masses were obtained prior to or subsequent to plate volume determinations, and these data are listed in Table 2. When the plot of these data, Fig. 8, is extrapolated to zero void volume, the clean critical mass is found to be 10.35 kg of U-235 for a metal volume of 19.7%.

Table 2. Critical Mass as a Function of Void Volume of Fuel Plates

Critical Mass (kg of U-235)	Void Volume (cm <sup>3</sup> )
10.45	2325
10.46	2361
10.55	4363

#### Critical Mass with Boron Poison

To obtain long core life, the APPR incorporates boron in the fuel elements as a burnable poison. The critical experiments included, therefore, the determination of the critical mass of the assembly as a function of the boron loading. The boron was introduced into the assembly in plates containing B<sub>4</sub>C in an iron matrix which was clad with stainless steel. Two types of plates were available; full plates containing 1.889 g of natural boron per plate and half plates containing 0.944 g of natural boron per plate. These data are given in Table 3, and the critical mass is plotted as a function of boron loading in Fig. 9. Note that no correction is made for fuel plate puffing. Heterogeneity effects in boron distribution are shown by comparing the critical mass for identical boron loadings in which half plates were substituted for some full plates.

### III. FUEL EVALUATION

The importance of an increment of fuel to the over-all reactivity of a reactor is dependent upon its location in the core and upon the average fuel density in the core. The value of fuel, averaged over the core, is a necessary parameter for conversion of excess reactivity to mass units or vice versa. Fuel evaluations were made in the assembly as a function of these variables.

~~CONFIDENTIAL~~

ORNL-LR-DWG 13547

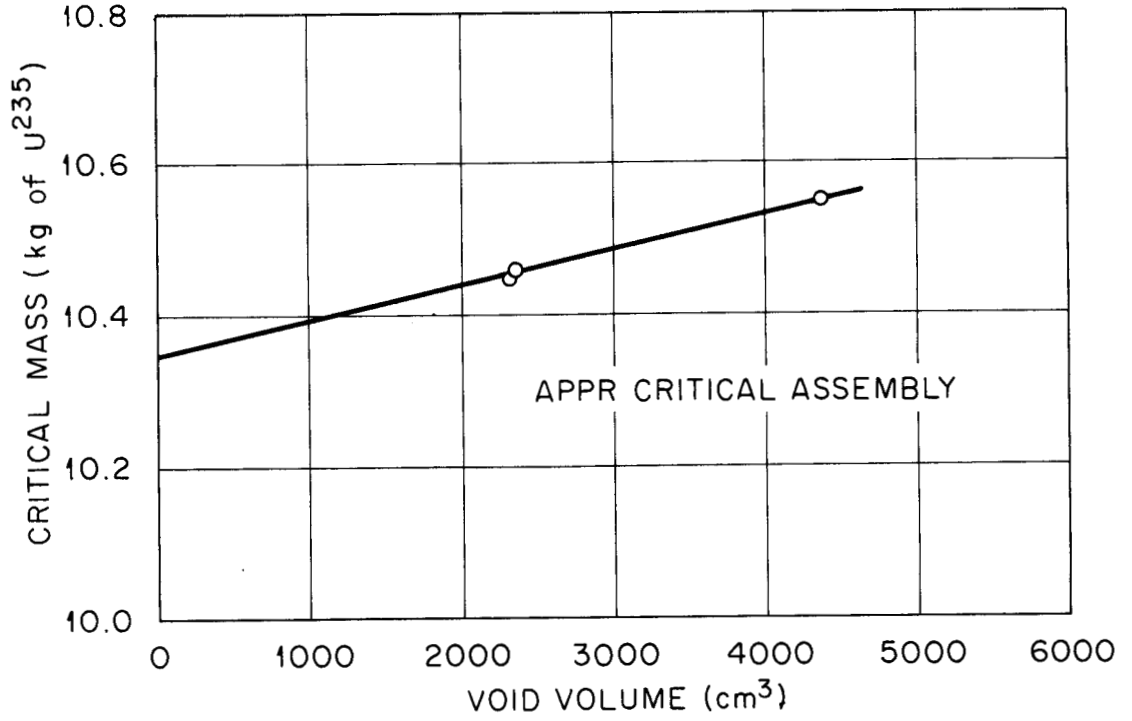


Fig. 8. Critical Mass as a Function of Void Volume of Fuel Plates.

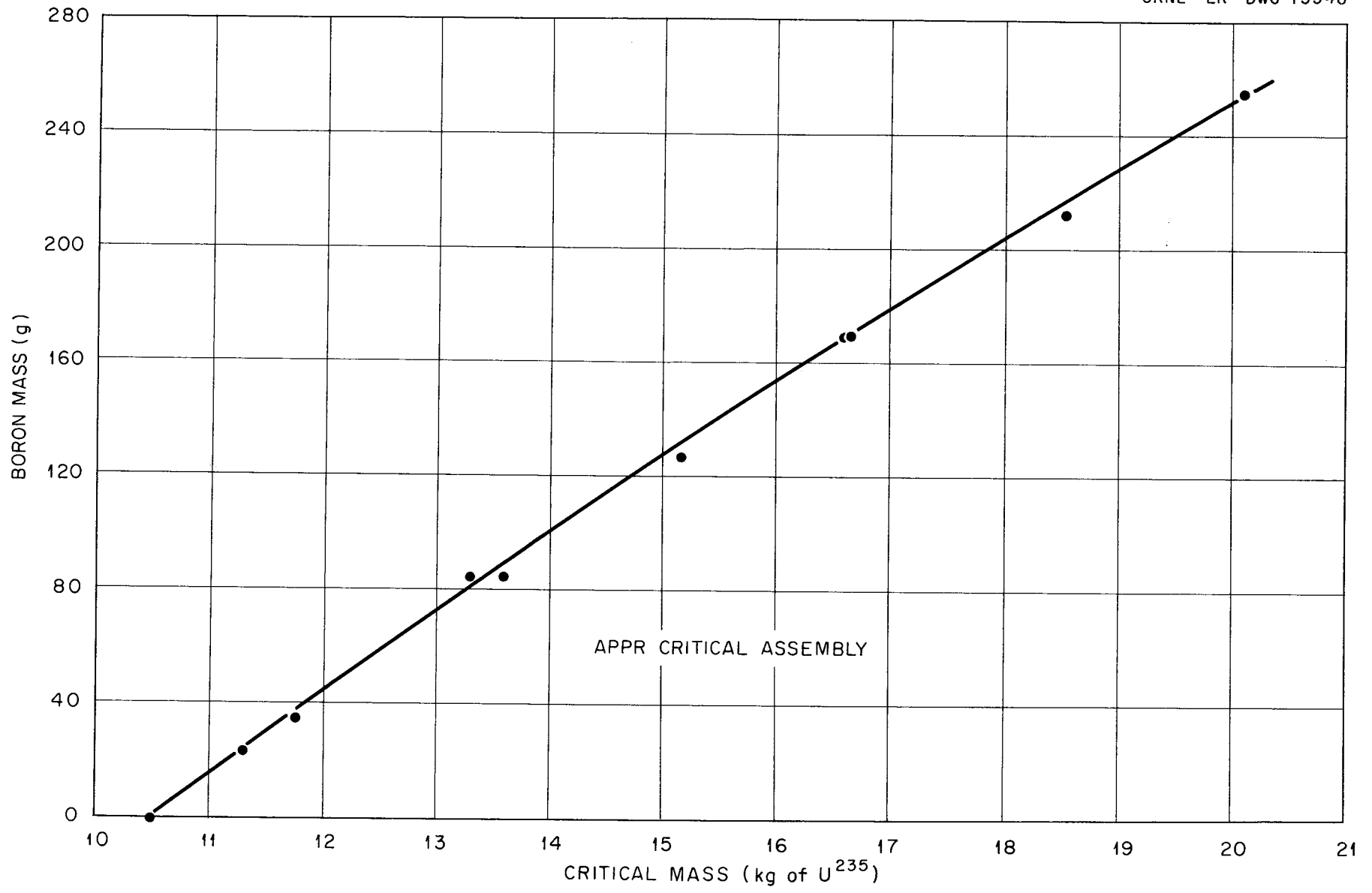


Fig. 9. Critical Mass as a Function of Boron Loading.

Table 3. Critical Mass as a Function of Boron Loading

Description of Boron Plate Distribution	Total Boron Mass (g of Natural Boron)	Critical Mass (kg of U-235)
1. No boron plates	0.0	10.50
2. Half plate in 24 elements	22.7	11.32
3. Half plate in 37 elements	34.9	11.76
4. Full plate in each element	85.0	13.30
5. Full plate in 22 elements; two half plates in 23 elements	85.0	13.60
6. One full and one half plate in each element	127.5	15.18
7. Two full plates in each element	170.0	16.63
8. Two full plates in all elements except No. 23 which contains four half plates	170.0	16.67
9. Two full and one half plates in each element	212.5	18.52
10. Three full plates in each element	255.0	20.10

Radial Fuel Importance

In the clean critical reactor the radial fuel importance was measured by replacing a stainless steel plate with either a half or a full fuel plate near the middle of each of the boxes 23, 16, 9 and 3, and noting the change in the control blade position to maintain the system critical. To minimize the errors of reactivity shifts because of puffed fuel plates, the reactor was returned to a reference condition between each measurement, and a plot of the control blade position vs time was used to obtain the correct reference blade position for each measurement. At this time the control blade was calibrated by means of positive periods so that the conversion from control blade position to reactivity in cents was quite accurate. It was necessary to evaluate full fuel plates near the center of the core in two steps; i. e., stainless steel

plate to half fuel plate and half fuel plate to full fuel plate, because a full plate was worth more than the control blade. These data are given in Table 4 and are shown in Fig. 10.

Table 4. Radial Fuel Evaluation

Location Element Slot	Steel Plate to Half Fuel Plate Value		Half Fuel Plate to Full Fuel Plate Value (cents)	Steel Plate to Full Plate Value		Average Value of Fuel (cents/g)
	(cents)	(cents/g)		(cents)	(cents/g)	
3 3	-	-	-	6.4	0.21	0.21
3 8	3.6	0.23	-	6.2	0.20	0.215
9 8	9.5	0.61	-	18.7	0.60	0.605
16 8	16.6	1.07	16.0	32.6 <sup>a</sup>	1.05	1.06
23 8	19.1	1.23	20.6	39.7 <sup>a</sup>	1.28	1.255
Average (r-weighted)						0.526

a. Not measured but the sum of the two parts.

From the above data a fuel value averaged over the core can be obtained. For a cylindrical reactor this average is

$$\bar{p} = \frac{\int_0^R 2\pi p(r) r dr}{\int_0^R 2\pi r dr} = \frac{2}{R^2} \int_0^R p(r)r dr$$

in which R is the core radius. Graphical integration over an average radius of 10.3 in. gives

$$\bar{p} = 0.526 \text{ cents/g}$$

This average corresponds to the value at a radius of 6.6 in.

Determinations of the Specific Mass Reactivity Coefficient

As stated previously, the critical loading of the reactor was varied between 10.51 and 20.10 kg of U-235 by the addition of boron plates. At each critical loading the same fuel plate containing 15.55 g of U-235 was removed near the middle of element 25 and the change in reactivity noted. The resulting values of the specific mass reactivity coefficient,  $m_{\Delta k}/k_{\Delta m}$ , are listed in Table 5 and are plotted in Fig. 11 as a function of the critical mass. These values are not necessarily representative of the entire core since the location of an "average" plate was not known as the boron loading was increased. In the clean reactor, item 1 of Table 5, the fuel value in

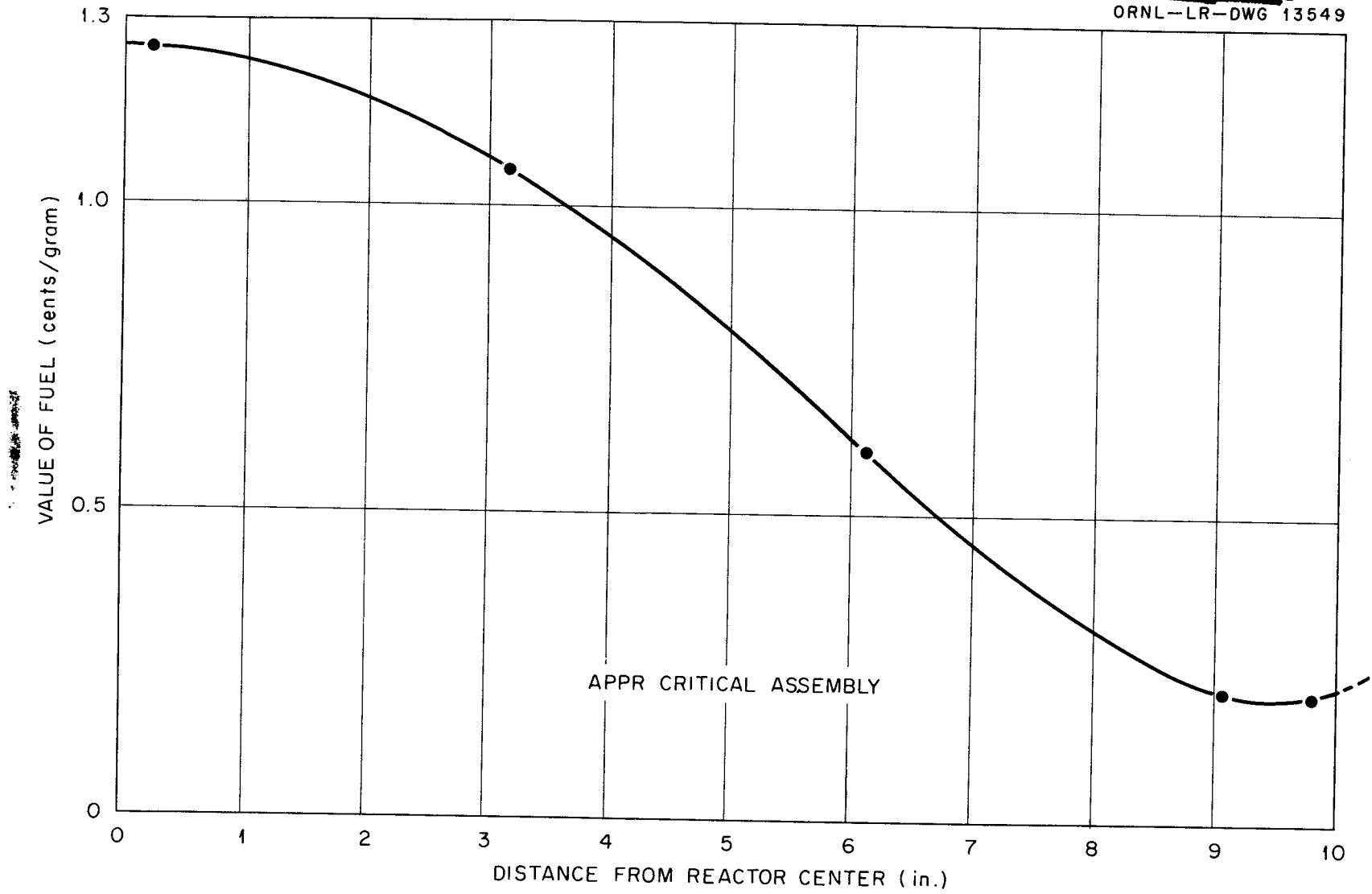


Fig. 10. Radial Fuel Evaluation.

Table 5. Specific Mass Reactivity Coefficient for Several Critical Loadings

Critical Mass (kg of U-235)	Change in Reactivity, $\Delta k$ , Due to $\Delta m = 15.55$ g (cents)	$\frac{\Delta k/k^a}{\Delta m/m}$
10.51	10.8	0.551
13.31	6.4	0.414
15.19	5.4	0.398
16.67	4.5	0.364
18.54	3.8	0.342
20.10	3.3	0.322

a. An effective delayed neutron fraction of 0.00755 was used to convert cents to  $\Delta k/k$ .

the above position is 32% higher than the average value of 0.526  $\text{¢/g}$  which indicates the other values in Table 5 are also probably higher than their respective core average values. In the absence of the effects of heterogeneity the specific mass reactivity coefficient averaged over the core is expected to be constant with variations of fuel loading. It is seen from Fig. 11 that this is approximately true for the critical experiment measurements.

#### IV. EFFECTS OF HETEROGENEITY ON CRITICAL MASS

The clean critical mass found for this assembly (10.35 kg of U-235) should differ significantly from the critical mass of a reactor made up of APPR-type elements because uranium and steel are distributed somewhat differently. To measure these effects two types of special elements were utilized, a homogeneous element which contained  $\text{UO}_2\text{F}_2$  in aqueous solution and an APPR-type element which contained uranium in a stainless steel matrix in 18 sandwich-constructed plates. These elements were exchanged with normal assembly elements in several locations, and the resulting positive changes in reactivity were measured.

##### Homogeneous Element

The homogeneous element was made from an assembly box containing 18 stainless steel plates on which a top and bottom were welded in order to make a watertight box 22 in. high. The box was filled with a  $\text{UO}_2\text{F}_2$  (~93% U-235) aqueous solution. Three different masses of uranium were put in the box: 227.5, 451 and 388 g of U-235. The 227.5-g homogeneous element was substituted for a 233-g (seven full and one half fuel plates) normal

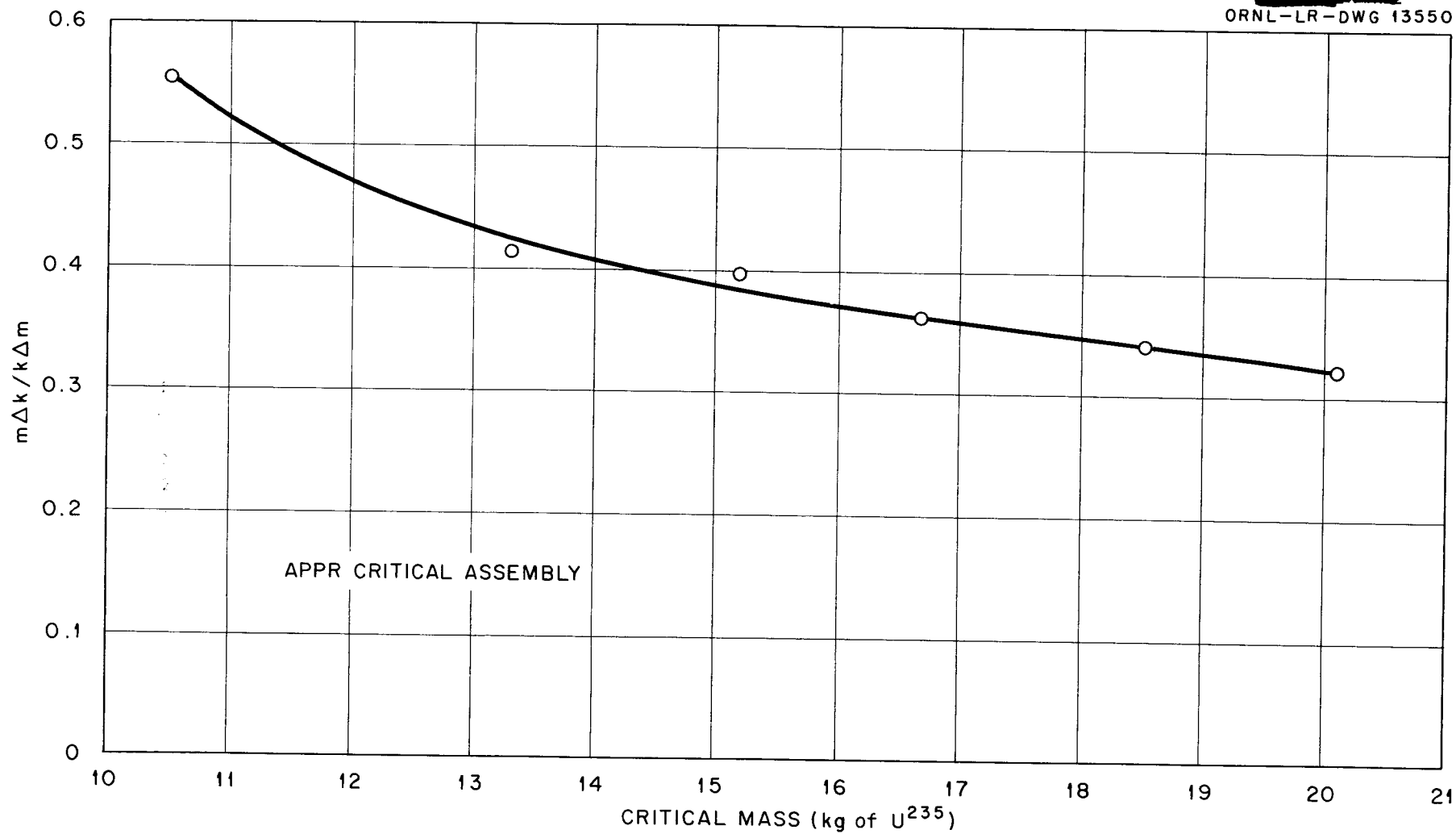


Fig. 11. Specific Mass Reactivity Coefficient for Several Critical Loadings.

assembly element in the clean core in positions 23, 37, and 43, and the resulting changes in reactivity were measured. The 451-g and the 388-g homogeneous elements were substituted for a 451-g unpoisoned normal assembly element in a core in which all other elements contained three full boron plates. For these experiments, the average fuel density for the remainder of the core was decreased from 451 g/element to compensate for the removal of three boron plates in the element for which the substitution was planned. The measured reactivity changes are given in Table 6.

Table 6. Reactivity Changes Effected by Homogeneous Element Substitutions

Type of Substitution	Reactivity Change (cents)			
	Position 23	Position 37	Position 43	Average Position
227.5 g homogeneous element in clean core	+ 55.3	+26.2	+ 7.8	+20.6
451 g homogeneous element in boron-loaded core	+ 50.2	+31.8	+18.8	-
388 g homogeneous element in boron-loaded core	+ 18.8	-	0.0	-

APPR-Type Element

The box for the APPR-type element<sup>7</sup> was formed by two grooved stainless steel side plates, 0.050 in. thick, joined by six small steel strips instead of end plates. For the complete APPR-type element eighteen fuel plates fitted into the grooves, which were separated 0.164 in. These plates contained a 22.0 x 2.5 x 0.020 in. stainless steel and uranium oxide matrix which was clad with stainless steel, 0.005 in. thick. Two sets of plates were made: one set contained 11.67 g of U-235 per plate, a total of 210 g per element, or 90% of clean critical assembly elements; the other contained 22.4 g of U-235 and 0.21 g of natural boron per plate or a total of 404 g of U-235 and 3.78 g boron per element. The 210-g APPR-type element was substituted for a 233-g (7-1/2 fuel plates) unpoisoned assembly element; the 404-g APPR-type element was substituted for an element containing 404 g of U-235 (13 full fuel plates) and 3.78 g of boron (two boron plates). The reactivity changes resulting from these substitutions are given in Table 7.

Table 7. Reactivity Changes Effected by APPR-Type Element Substitutions

Type of Substitution	Reactivity Change (cents)			
	Position 23	Position 37	Position 43	Average Position
210 g element	+11.3	+6.9	+2.5	+5.26
404 g element with boron	+26.6	+14.7	+9.4	+13.4

Analysis of Heterogeneity Effects

The calculation from these data of the critical mass of a reactor that would be made up entirely of the special elements involves the assumption that the average fuel worth,  $\bar{p}$ , varies inversely as the fuel mass (or fuel density).

$$\bar{p}_1 M_1 = \bar{p}_2 M_2$$

As fuel is added to a reactor homogeneously, the plot of the excess reactivity,  $\rho$ , vs total mass,  $M$ , can be used to define the fuel worth which is the slope at any point. This equation is

$$\left( \frac{d\rho}{dM} \right)_{M_1} = \bar{p}_1$$

The total excess reactivity in a reactor consisting entirely of special elements is equal to the integration of the equation which defines fuel worth between the mass limits of  $M_x$  and  $M_0$

$$\int_0^{M_x} d\rho = \bar{p}_0 M_0 \int_{M_0}^{M_x} \frac{dM}{M}$$

or

$$\rho = \bar{p}_x M_x \ln \frac{M_x}{M_0}$$

- $M_x$  = mass of a reactor consisting entirely of special elements,
- $M_0$  = mass of the same reactor corrected to zero excess reactivity,
- $\bar{p}_x$  = average value of the special element fuel.

A reactivity balance for the substitution of a special element is

$$p_x(r)m_x = \rho(r) + p_n(r)m_n$$

in which

$$\begin{aligned}
 m_x &= M_x/45, \\
 m_n &= \text{mass of U-235 in critical experiment fuel element,} \\
 p_n(r) &= \text{fuel value at } r \text{ in critical experiment fuel element.}
 \end{aligned}$$

Averaging the r dependent quantities, the equation becomes

$$\bar{p}_x m_x = \bar{p} + \bar{p}_n m_n$$

therefore

$$\bar{p} = \bar{p}_x m_x \ln \frac{M_x}{M_0} = (\bar{p} + \bar{p}_n m_n) \ln \frac{M_x}{M_0}$$

The useful form of the equation is obtained by rearrangement:

$$M_0 = M_x \exp\left(-\frac{\bar{p}}{\bar{p} + \bar{p}_n m_n}\right)$$

The calculations of  $M_0$  for various types of elements from the above equation are listed in Table 8.

Table 8. Critical Mass of Cores Consisting of Special Elements

Type of Substitution	Critical Mass for Core Consisting of Special Elements (kg of U-235)
Homogeneous element in clean core <sup>a</sup>	8.87
APPR element in clean core	9.07
APPR element in boron-loaded core	16.47

a. The homogeneous element core can not be considered the same as a completely homogeneous core because of flux peaking between elements.

Figure 12 shows these calculated critical mass values of the reactor as well as the experimental values as a function of boron loading. This figure illustrates the magnitude of heterogeneity effects for various uranium loadings; the effect is quite pronounced at the lower masses but as more fuel plates are loaded into the assembly elements, the effect becomes negligible.

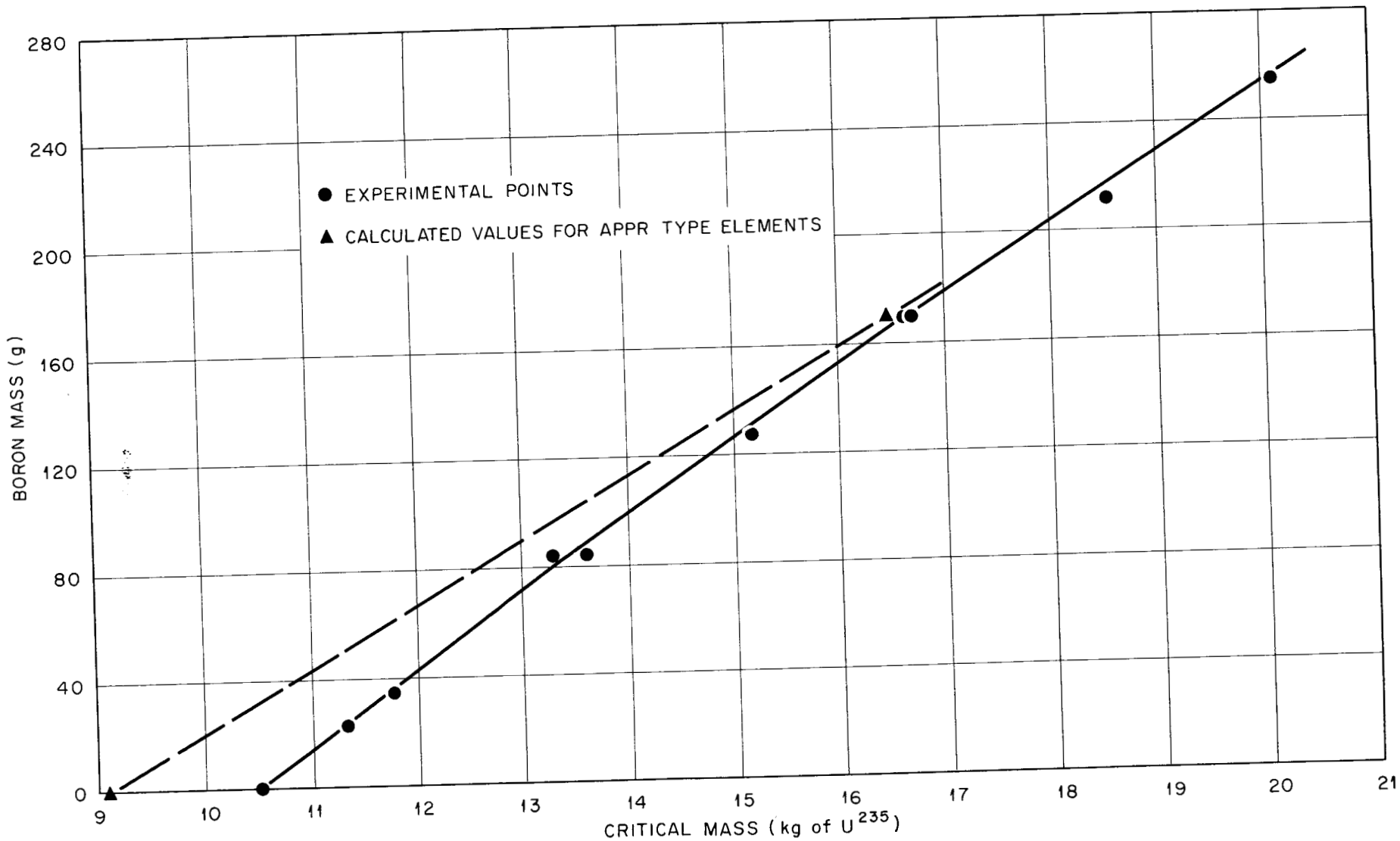


Fig. 12. Calculated Critical Mass of APPR as a Function of Boron Loading.

## V. APPR CONTROL ROD EVALUATIONS

The control rods used in the critical experiment have been described in detail earlier in this report. They are constructed in two sections, a poison section 22 in. long separated 2 in. from the top of the fuel in a section which is similar to the other fuel boxes of the critical assembly. A total motion of 24 in. resulted in moving the bottom of the poison section of the rod from the bottom of the core, position 0.0 in., to a position 2 in. above the core, position 24.0 in., in which the fuel section was aligned in the core. The APPR was designed to have control rods in positions 9, 21, 23, 25 and 37.<sup>1</sup> In order to provide information for APPR-1 design some comparisons were made of the values of the rods in the above positions with values of the five rods in a more closely packed array in positions 15, 17, 23, 29 and 31. As a result of these measurements it has been proposed that reserve control rods<sup>11</sup> be located in positions 15 and 31 in addition to the original five, and critical masses were measured with varying amounts of U-235, boron and stainless steel in these seven positions consistent with APPR-1 design.

### Rod Measurements with Clean Core

The rod configurations were evaluated by adding uranium plates to the core to achieve criticality, and the rod values were expressed as the amount of uranium in excess of the clean critical mass. These data are summarized in Table 9 in which the mass includes the fuel in the control rods. The addition of the fuel section to rod 23 alone or the addition of fuel sections to rods 9, 21, 23 and 25 collectively resulted in less than  $\pm 5\%$  change in reactivity in both cases.

The equation  $\rho = \bar{\rho}_0 M_0 \ln(M/M_0)$  from the previous section was used in calculations of the reactivity value for each of the mass loadings for the different control rod configurations, and these rod values in dollars are also listed in Table 9. A plot of the mass worth as a function of the position of the five ganged control rods is presented in Fig. 13. This graph shows the extreme asymmetry of the ganged rods. The interaction of rods is illustrated by comparing the value of the combination to the sum of its parts. This ratio is given in Table 10 for several configurations using \$4.0 and \$8.9 for the individual values of the eccentric and central rods, respectively.

---

11. J. L. Meem, private communication.

Table 9. Mass and Reactivity Values of Various Rod Configurations in the Clean Core

Location in Core	Rod Configuration	Vertical Position <sup>a</sup> (in.)	Experimental Critical Mass (kg of U-235)		Mass Value of Rods (kg of U-235)	Estimated Reactivity (dollars)
			Clean Without Rods	With Rods		
	37	0.0	10.49	11.17	0.68	4.0
	23	0.0	10.49	12.18	1.69	8.9
	23	0.0	10.59	12.31	1.72	9.0
	37	7.3	10.59	12.31	1.72	9.0
	9	0.0				
	23, 37	0.0	10.49	13.05	2.56	12.7
	23, 31	0.0	10.49	13.25	2.76	13.6
	25, 37	0.0	10.49	12.07	1.58	8.4
	9, 21, 23, 25	0.0	10.59	16.77	6.18	26.8
	9, 21, 23, 25	0.0	10.55	17.24	6.69	28.4
	37	18.0				
	9, 21, 23, 25	0.0	10.55	18.61	8.06	32.6
	37	12.4				
	9, 21, 23, 25	0.0	10.55	18.65	8.10	32.8
	37	12.0				
	9, 21, 25, 37	0.0	10.55	17.31	6.76	28.6
	9, 21, 25, 37	0.0	10.55	18.66	8.11	32.8
	23	12.1				
	9, 21, 25, 37	11.9	10.55	12.55	2.00	10.6
	23	11.9				
	9, 21, 25, 37	6.5	10.59	17.48	6.89	29.2
	23	6.5				
	9, 21, 25, 37	0.0	10.59	22.82	12.23	44.1
	23	0.0				

a. At 0.0 in. the boron section is completely in the reactor and at 24.0 in. the fuel section is completely in the reactor.

ORNL-LR-DWG 13552

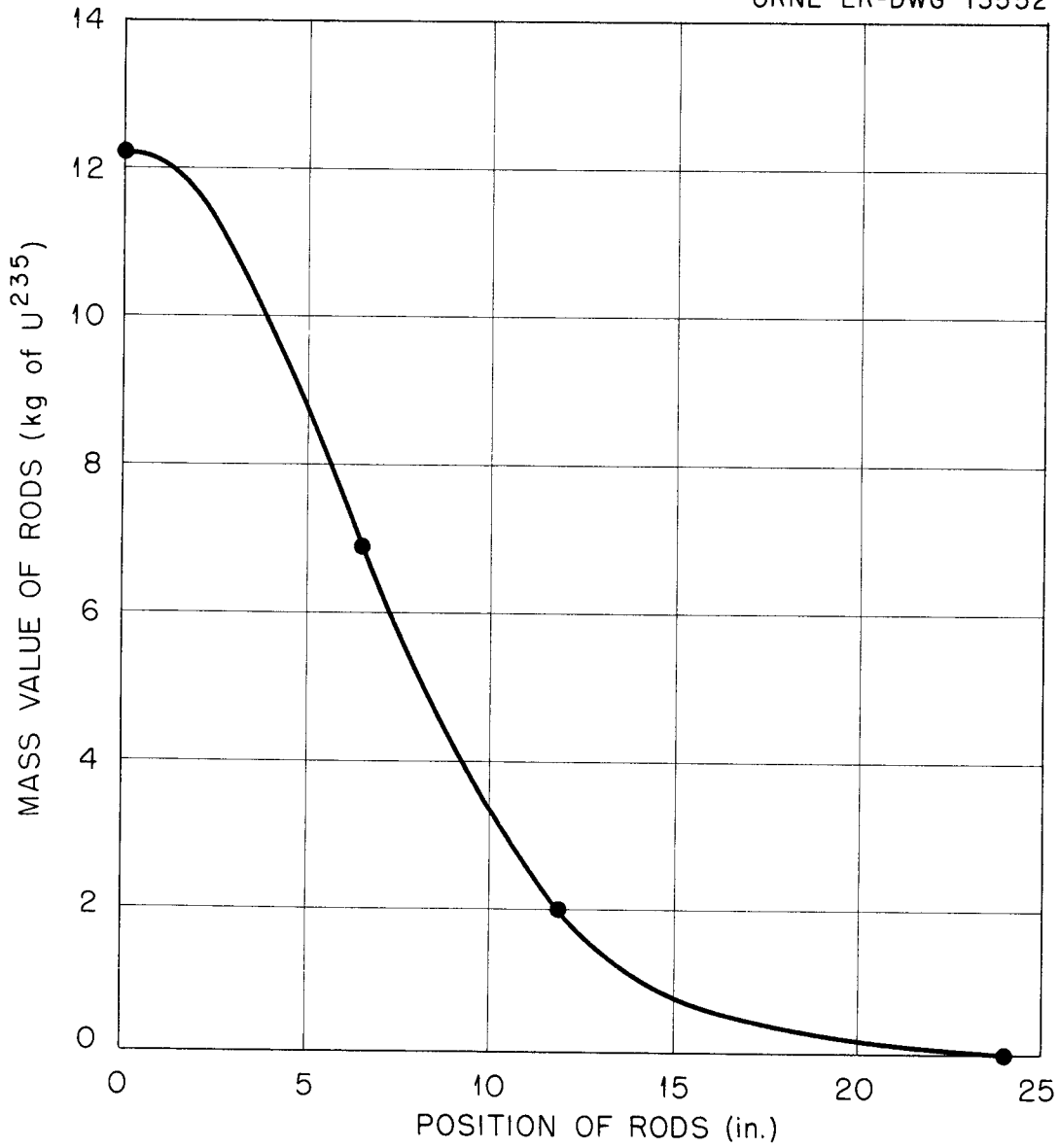


Fig. 13. Calibration of Five Ganged APPR Control Rods.

Table 10. Rod Interactions

Rod Configuration	Reactivity (dollars)		Ratio
	Combined Value of Rods	Sum of Component Rod Values	
23, 37	12.7	12.9	0.98
25, 37	8.4	8.0	1.05
9, 21, 23, 25	26.8	20.9	1.28
9, 21, 25, 37	28.6	16.0	1.59
9, 21, 23, 25, 37	44.1	24.9	1.77

Calibration of Eccentric Rod No. 37

In addition to the mass evaluation of the APPR control rods, it was desirable to have a direct measurement of the reactivity of one of the APPR control rods in the critical experiment. Since it was impossible to perform a rod drop experiment because of the structural design, a comparison of rods 9 and 37 was made in small increments. Each of the increments was measured as a positive or negative period or the sum of both. Initially the reactor was critical with rod 9 fully inserted and rod 37 fully withdrawn. Rod 9 was jogged out, and the resulting positive period was measured. Rod 37 was inserted until a suitable negative period was achieved and measured. Rod 9 was jogged out until the desired positive period was obtained and measured. This rod comparison was continued until the rod positions were reversed. The inhour equation was used to convert the periods to cents. These data are summarized in Table 11, and the rod calibration curve is presented in Fig. 14.

Rod Measurements with Boron-Poisoned Core

Some information concerning the value of the control rods in a reactor which contained distributed boron poison was obtained. Four control rods, in positions 9, 21, 23 and 37, were inserted into the reactor which contained all of the available uranium plates, and the excess reactivity was compensated by the addition of distributed boron plates. This experiment was repeated with the eccentric rods moved to positions 15, 17 and 29. A third determination was made of the critical mass of a reactor which contained one boron plate per element and in which the five rods were half inserted. These data are listed in Table 12. It is interesting to note that the rods in the eccentric positions 15, 17, 23 and 29 are worth more than in the positions 9, 21, 23 and 37.

Table 11. APPR Rod No. 37 Calibration

Rod Position (in.)	Rod Value (cents)
24.08	0.0
21.40	14.1
19.54	32.7
18.27	54.0
16.99	81.2
16.02	104.3
15.09	128.1
14.20	152.7
13.36	175.5
12.59	198.0
11.88	218.0
11.11	239.4
10.30	261.0
9.40	284.3
8.09	314.8
6.74	339.9
5.14	360.2
3.75	370.7
0.10	380.6

Table 12. Mass Values of Various Rod Configurations in the Boron-Poisoned Core

Rod Configuration Location in Core	Vertical Position (in.)	Boron (g)		Critical Mass (kg of U-235)		Worth of Rods and Boron (kg U-235)	Worth of Boron Only <sup>a</sup> (kg U-235)
		In Core	In 45 Elements	Experi- Mental Clean	With Rods and Boron		
9,21,37 23	0.0 0.0	31.2	34.2	10.53	18.29	7.76	1.18
15,17,29 23	0.0 0.0	22.7	24.9	10.53	18.26	7.73	0.85
15,17,29,31	0.0	22.7	24.9	10.53	18.26	7.73	0.85
9,21,25,37 23	12.0 12.0	85.0	85.0	10.59	15.99	5.40	2.78

a. From Fig. 9, "Critical Mass vs Boron Loading."

~~CONFIDENTIAL~~  
ORNL-LR-DWG 13553

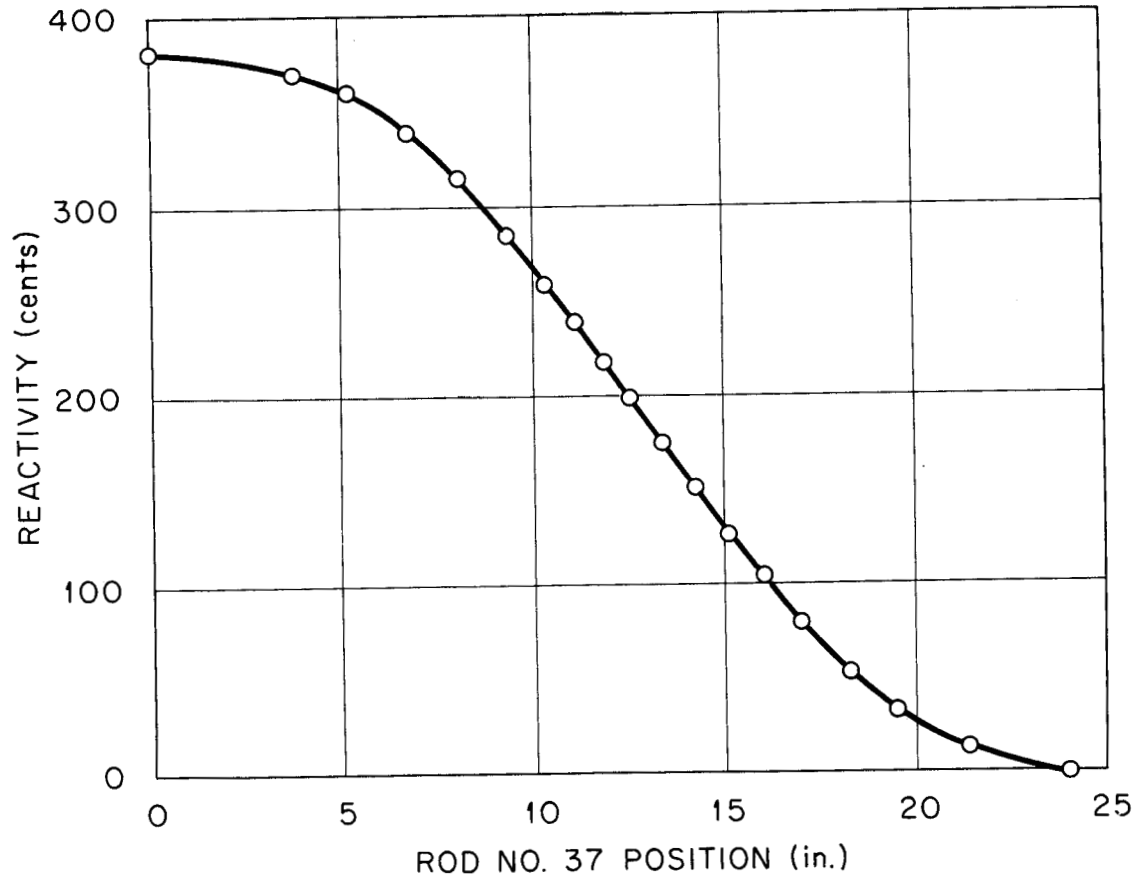


Fig. 14. APPR Rod No. 37 Calibration.

Mockup of APPR-1 Control Rods

The fuel section of the APPR-1 rods will contain about 20% less uranium and boron than the other fuel elements in the core and will have a metal volume of 22.6% compared to a normal APPR-1 fuel element of 20.5%.<sup>11</sup> An attempt was made to mock up the above condition in the critical experiment for the boron-loaded core. Fuel and boron were removed from rods 9, 15, 21, 23, 25, 31 and 37, and criticality was achieved by adding fuel to the remainder of the core. Steel was added to the same rods by inserting two steel plates in the same slot and by taping steel plates on the outside of the box, and the reactor made critical by removing boron from the other elements. These data are given in Table 13.

Table 13. Reactor Loading for the Mockup of the Seven APPR-1 Control Rods.

	Case 1	Case 2	Case 3
<b>Core Element</b>			
U-235 Mass (g)	447	466.5	466.5
Boron Mass (g)	5.7	5.7	5.5
Stainless Steel Mass (g)	4737	4737	4737
<b>Control Rod</b>			
U-235 Mass (g)	447	373.2	373.2
Boron Mass (g)	5.7	4.7	4.7
Stainless Steel Mass (g)	4737	4737	5518
<b>Mass Ratio: Control Rod/Core Fuel Element</b>			
U-235	1.00	0.80	0.80
Boron	1.00	0.833	0.85
Stainless Steel	1.00	1.00	1.16
<b>Critical Masses</b>			
U-235 Mass (kg)	20.10	20.00	20.33
Boron Mass (g)	255	248	241

VI. NEUTRON FLUX AND POWER DISTRIBUTION MEASUREMENTS

Description of Detectors

The macroscopic neutron flux distributions throughout the assembly were obtained using bare and cadmium-covered gold foils. These foils were 0.313 in. in diameter, 0.002 in. thick and weighed approximately 46 mg each. They were weight-grouped to the nearest 0.1 mg before using. The cadmium covers were 0.020 in. thick.

~~CONFIDENTIAL~~

Dysprosium, which is an approximate  $1/v$  detector of thermal neutrons and is activated only slightly by neutrons with energies above the cadmium cut-off,<sup>12</sup> was used for all microscopic, or intracell flux measurements. The foils were 0.242 in. in diameter and 0.011 in. thick, and they contained approximately  $1 \text{ mg/cm}^2$  of dysprosium oxide. The dysprosium oxide was mixed with electrically fused  $\text{Al}_2\text{O}_3$  and bonded by an organic resin. The half-life of the foils agreed with the 139.12-min value observed by Downes.<sup>13</sup> The activities induced in the foils upon exposure to the same neutron flux agreed to within  $\pm 2.5\%$ .

The gold and dysprosium foil activations were determined with Atomic Instrument Company Model 1010 binary scalers using Amperex Model 120-C mica-window Geiger tubes. Each side of every foil was counted 3-min in each of four counters, and the eight values were averaged after they had been corrected for dead-time, background, decay, and counter sensitivity.<sup>14,15</sup> The minimum number of observed counts for each foil was the order of  $10^5$ .

If an aluminum foil is in contact with uranium fuel while a reactor is in operation, the activity of the fission fragments collected on the aluminum is a measure of the fission rate at the surface of the fuel. All power distributions reported here were obtained by this "catcher foil" method. The diameters of the 0.005 in. thick 2S aluminum foils were 0.900 in. and 0.500 in. They were placed in contact with the uranium in special fuel plates having holes 1.00 in. in diameter at various vertical positions.<sup>4</sup> These holes were closed with an 0.011-in.-thick stainless steel disc and sealed with polyethylene tape. All catcher foils were exposed 20 min and counted in a Radiation Counter Laboratories methane gas flow proportional counter. Their activities were normalized to 60 min after shutdown using an empirically determined decay curve. The counting time for each catcher foil varied from 1.5 to 3 min which gave a minimum of  $10^5$  counts. Exposures were normalized for power variations by an appropriate foil, either aluminum, dysprosium or gold, located in the same position in the reactor.

## Results

A summary of all neutron flux and power distribution measurements is given in Table 14. This is followed by the tables and figures for the individual traverses which are self-explanatory.

Catcher foils, both bare and cadmium-covered, were exposed at the reactor midplane on the fuel in slot 10 of elements 3, 23, and 37 of the clean reactor. The fuel cadmium fraction, i. e., the fraction of fissions occurring below cadmium cut-off, for each of these locations was  $0.91 \pm 0.01$ . The dysprosium cadmium fraction was obtained in element 16 for both the clean and the 255-g boron-loaded reactors, and these values were 0.97 and 0.92, respectively.

12. "Neutron Cross Sections", BNL-325

13. K. Downes, private communication

14. E. L. Zimmerman, "A Graphite Moderated Critical Assembly, CA-4", Y-881, Appendix B, p. 66, (Dec. 7, 1952).

15. D. V. P. Williams, "Neutron Detection by Foils", University of Tennessee Thesis (Aug. 1955)

Table 14. Summary of Neutron Flux and Power Distribution Measurements

Type Traverse	Location <sup>a,b</sup>	Orientation with Respect fo Fuel	Reactor Conditions	Recorded in	
				Fig. No.	Table No.
Macroscopic Neutron Flux Using Gold Foils					
Horizontal	Midplane (23-3)	Perpendicular	Clean	15	15
			Boron loaded <sup>c</sup>	16	16
	Midplane (16-3)	Perpendicular	APPR rod No. 23 inserted	17	17
Vertical	Center of element 23	Parallel	Clean	18	18
			Clean with end boxes	19	18
	Center of element 30	Parallel	APPR rod No. 23 inserted	20	19
Macroscopic Power Using Fission Fragment Catcher Foils 0.9 in. Diameter					
Horizontal	Midplane (23-3)	Perpendicular	Clean	21	20
	Midplane (23-26)	Parallel	Clean	22	20
	Midplane (23-3)	Perpendicular	Boron-loaded	23	21
	Midplane (23-11)	Diagonal	Boron-loaded	24	22
	Midplane (16-3)	Perpendicular	APPR rod No.23 inserted	25	23
	13 in. from top of core (23-26)	Parallel	Five APPR rods half inserted <sup>d</sup>	26	24
	17 in. from top of core (23-26)	Parallel	Five APPR rods half inserted	26	24
	21 in. from top of core (23-26)	Parallel	Five APPR rods half inserted	26	24
Vertical	Center of element 23	Parallel	Clean	27	25
			Clean with end boxes	27	25
	Center of element 16	Parallel	APPR rod No. 23 inserted	27	25
	Center of element 23	Parallel	Boron-loaded	28	26
	West side of slot 18 in element 23	Parallel	Five APPR rods half inserted	29	27
	East side of slot 1 in element 16	Parallel	Five APPR rods half inserted	29	27
Microscopic Neutron Flux Using Dysprosium Foils					
Horizontal	Midplane (23-16)	Perpendicular	Clean	30	28
			APPR element in position No. 23	31	29
	Midplane (23-24)	Parallel	Clean	32	30
			APPR element in position No. 23	32	30

Table 14. (cont.)

Type Traverse	Location <sup>a,b</sup>	Orientation with Respect to Fuel	Reactor Conditions	Recorded in	
				Fig. No.	Table No.
Horizontal	Midplane (23-16)	Perpendicular	Boron-loaded	33	31
	Midplane (23)	Periphery of element	Boron-loaded	34	32
Microscopic Power Using Fission Fragment Catcher Foils 0.5 in. in Diameter					
Horizontal	South edge of element 5 at midplane	Perpendicular	Clean	35	33
	East side, slot 1 of element 12 at midplane	Parallel	Clean	35	33

- a. "Midplane (23-3)" means that traverse was in the midplane of the reactor extending from element 23 through element 3.
- b. Center of element is defined here as east side of Slot 10 (see Fig. 5).
- c. Boron-loaded reactor has 255 g of natural boron distributed throughout core.
- d. Five APPR rods in positions 9, 21, 23, 25 and 37.

Table 15. Horizontal Flux Distribution in Clean Reactor.

Traverse at midplane perpendicular to fuel plates.

Distance from Reactor Center (in.)	Gold Foil Relative Activity		
	Bare	Cadmium-Covered	Cadmium Fraction
- 0.07	1.000	0.492	0.508
0.96	0.991	0.490	0.506
2.43	0.993	0.456	0.541
3.91	0.866	0.426	0.508
5.39	0.804	0.394	0.510
6.42	0.665	0.322	0.516
7.60	0.558	0.278	0.502
8.78	0.468	0.213	0.545
10.11	0.375	0.135	0.640
11.44	0.684	-	-
12.44	0.531	0.0472	0.91
13.44	0.369	0.0246	0.93
14.44	0.226	0.0145	0.94
16.44	0.0822	0.0044	0.95
18.44	0.0276	0.002	-
20.44	0.0108	0.001	-

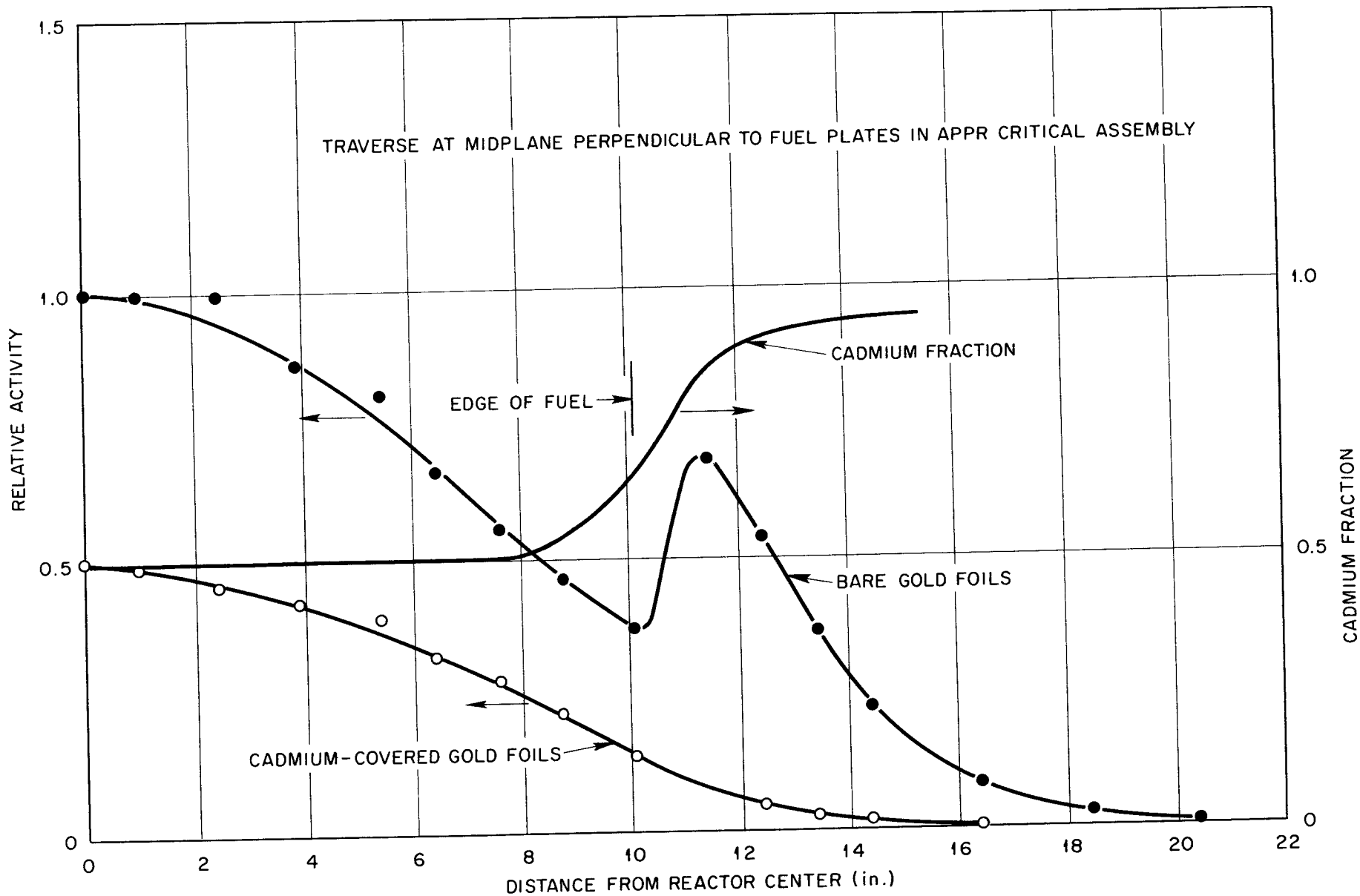


Fig.15. Horizontal Flux Distribution in Clean Reactor.

Table 16. Horizontal Flux Distribution in Reactor Containing  
255 g of Boron.

Traverse at midplane perpendicular to fuel plates.

Distance from Reactor Center (in.)	Gold Foil Relative Activity	
	Bare	Cadmium-Covered
0.52	1.0111	0.7188
1.26	1.1790	0.7168
3.47	0.9700	0.6400
4.21	1.0059	0.6137
6.42	0.6963	0.4900
7.16	0.6971	0.4431
9.37	0.4117	0.2731
10.11	0.4894	0.2134
11.44	1.0362	0.1309
12.44	0.8414	0.0700
13.44	0.5711	0.0411
14.44	0.3611	0.0229
15.44	0.2168	0.0143
16.44	0.1277	0.0080
17.44	0.0463	0.0054

Table 17. Horizontal Flux Distribution in Clean Reactor with  
Central APPR Rod Inserted.

Traverse at midplane perpendicular to fuel plates.

Distance from Reactor Center (in.)	Gold Foil Relative Activity		
	Bare	Cadmium-Covered	Cadmium Fraction
1.69	0.577	0.346	0.400
2.29	0.792	0.421	-
2.88	0.886	0.471	0.472
3.47	0.977	0.486	-
4.21	1.000	0.504	0.500
5.24	0.935	0.492	-
5.83	0.911	0.487	0.492
6.87	0.852	0.439	-
7.89	0.734	0.383	0.483
8.78	0.627	0.320	0.490
10.11	0.571	0.213	0.627
11.44	1.053	0.125	0.881
12.44	0.839	0.068	0.919
13.44	0.548	0.038	0.931
15.44	0.206	0.014	0.932

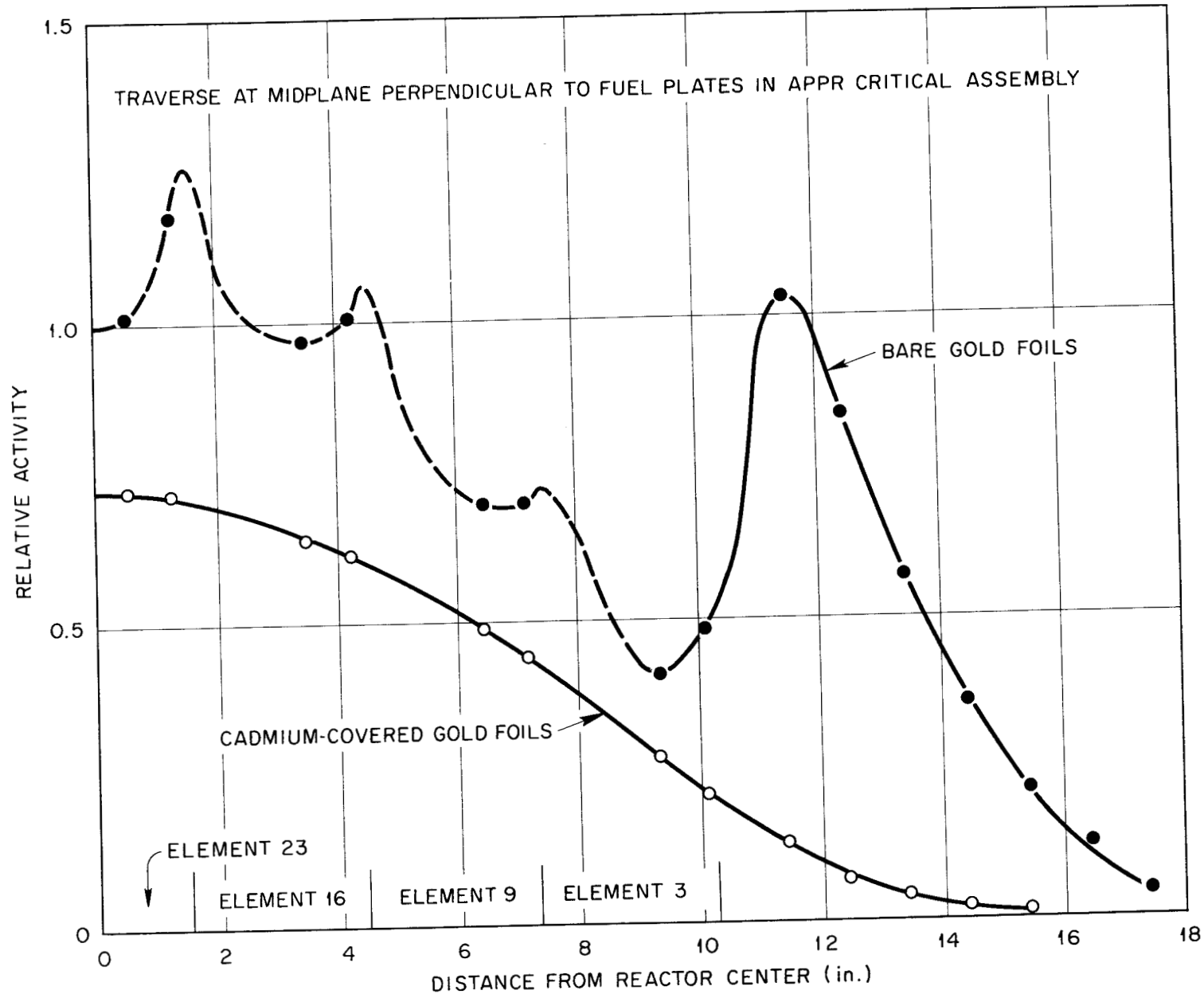


Fig. 16. Horizontal Flux Distribution in Reactor Containing 255 g of Boron.

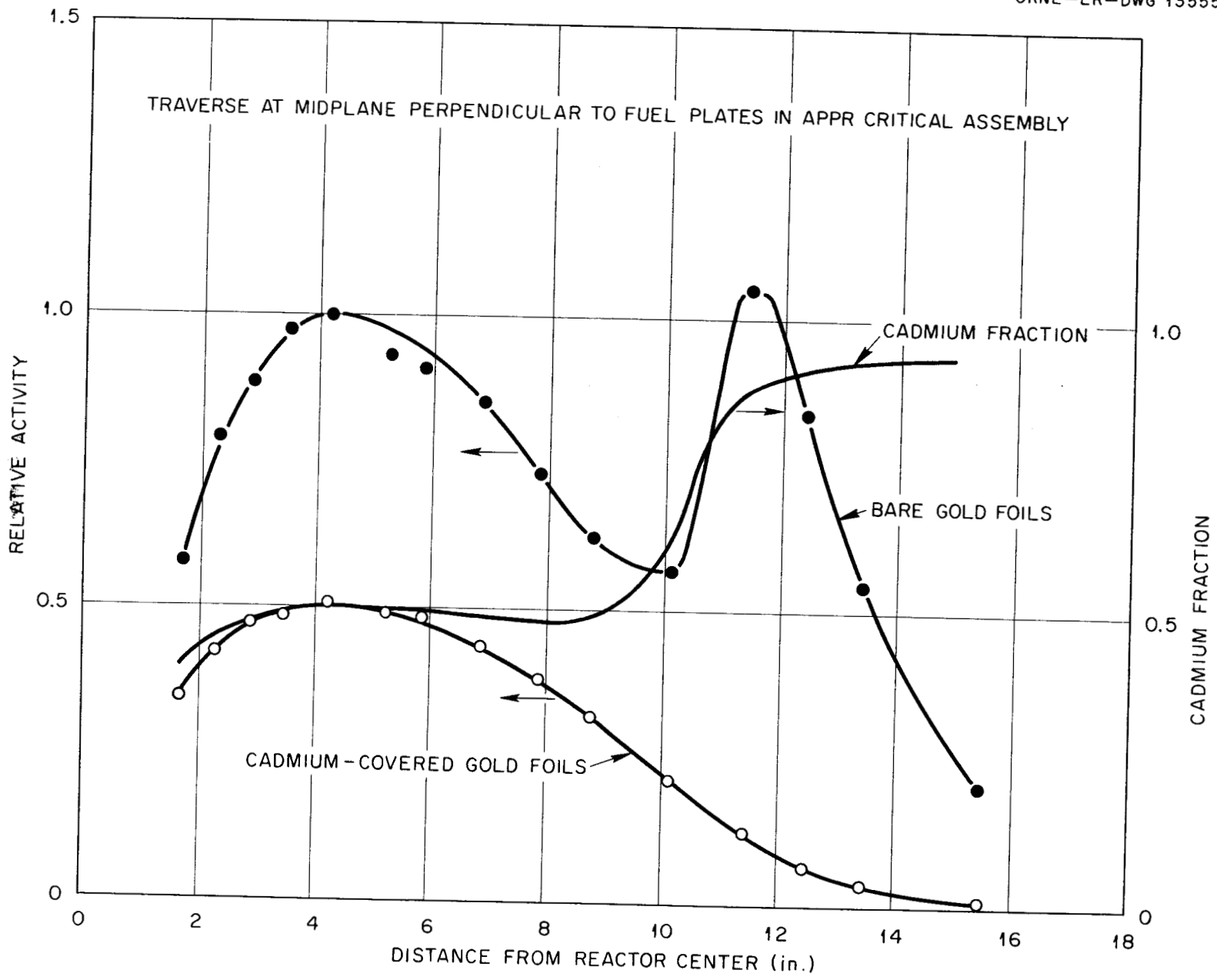


Fig. 17. Horizontal Flux Distribution in Clean Reactor with Central APPR Rod Inserted.

Table 18. Vertical Flux Distributions in Element 23 of Clean Reactor

Distance above Reactor Midplane (in.)	Gold Foil Relative Activity		
	Bare	Cadmium- Covered	Cadmium Fraction
Without End Boxes			
0.00	1.000	0.459	0.541
1.50	0.965	0.466	0.517
3.00	0.923	0.451	0.511
4.50	0.835	0.406	0.514
6.00	0.714	0.348	0.513
7.50	0.601	0.291	0.517
9.00	0.457	0.225	0.507
10.00	0.368	0.170	0.538
10.88	0.344	0.124	0.640
11.18	0.414	0.110	0.735
11.35	-	0.105	-
11.85	0.531	0.083	0.84
12.50	0.469	0.057	0.88
13.50	0.332	0.032	0.90
15.00	0.188	0.013	0.93
16.50	0.090	0.0051	0.94
18.50	0.014	0.0016	-
With End Boxes			
0.00	1.000	0.454	0.547
1.50	0.973	0.447	0.541
3.00	0.941	0.423	0.551
4.50	0.849	0.396	0.533
6.00	0.746	0.339	0.545
7.50	0.622	0.286	0.540
9.00	0.475	0.215	0.548
10.85	0.358	0.128	0.641
11.78	0.505	0.090	0.82
12.50	0.426	0.066	0.85
13.50	0.227	0.039	0.83
15.00	0.093	0.018	0.81
17.00	0.024	0.007	0.71

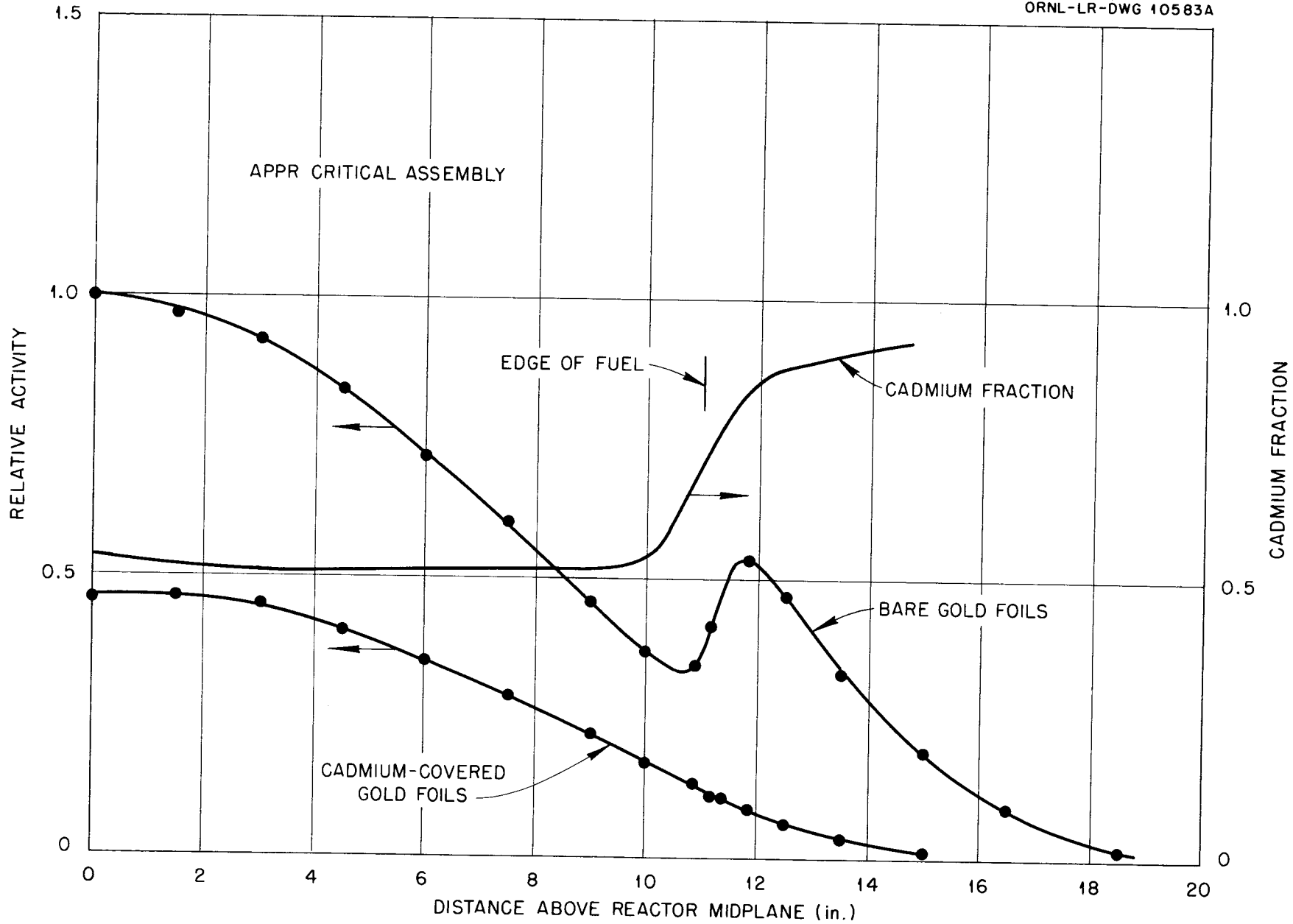


Fig. 18. Vertical Flux Distribution in Element 23 of Clean Reactor without End Boxes.

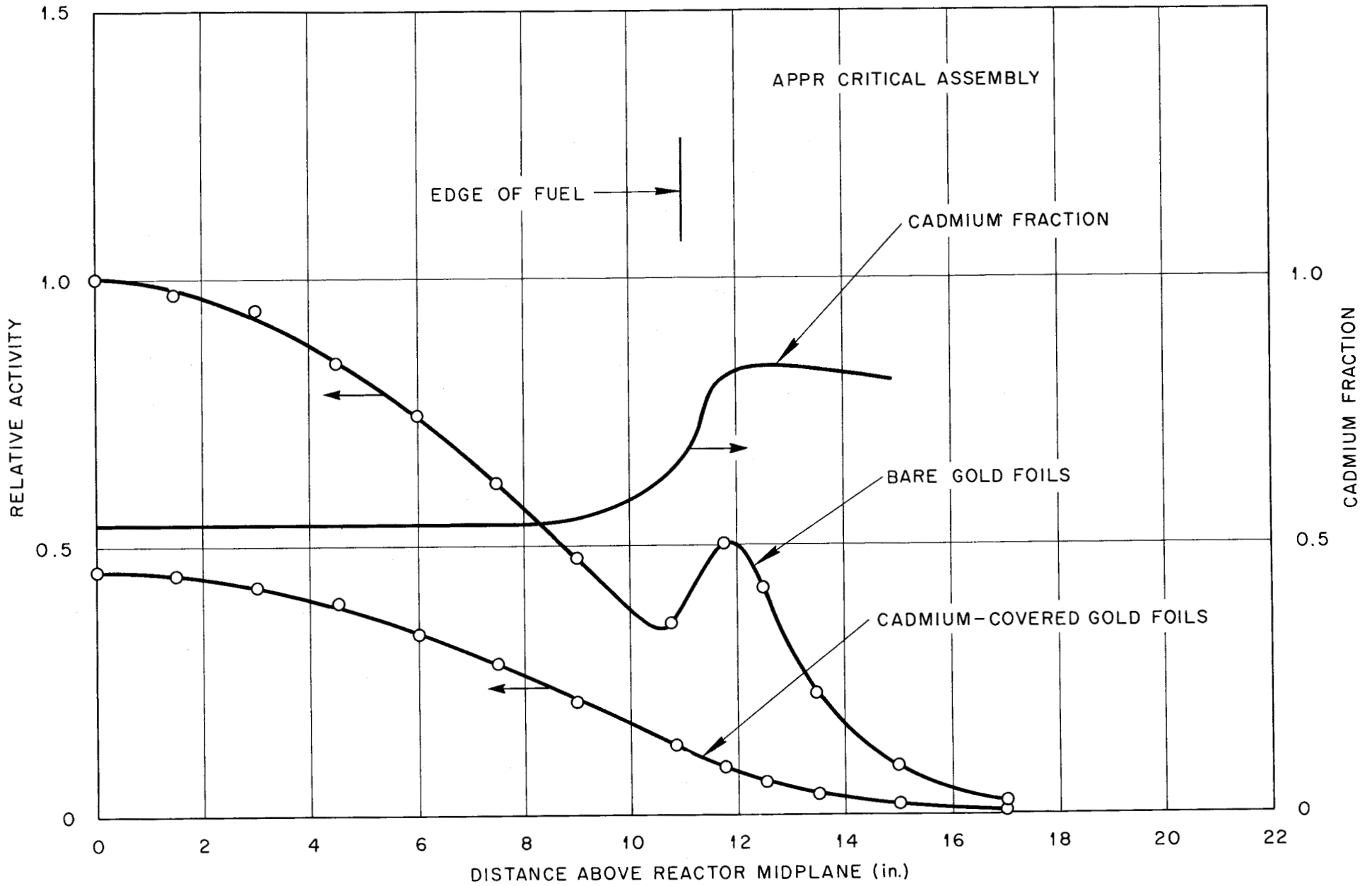


Fig. 19. Vertical Flux Distribution in Element 23 of Clean Reactor with End Boxes.

Table 19. Vertical Flux Distribution in Element 30  
of Clean Reactor with Central APPR Rod Inserted

Distance above Reactor Midplane (in.)	Gold Foil Relative Activity		
	Bare	Cadmium Covered	Cadmium Fraction
0.00	1.000	0.513	0.487
2.00	0.986	0.503	0.490
4.00	0.858	0.458	0.466
6.00	0.728	0.383	0.474
8.00	0.558	0.295	0.471
10.00	0.382	0.196	0.487
11.31	0.499	0.128	0.745
12.00	0.539	0.102	0.81
13.00	0.359	0.059	0.84
15.00	0.118	0.023	0.80
17.50	0.020	0.012	-

Table 20. Horizontal Power Distribution at Midplane  
in Clean Reactor

Perpendicular to Fuel Plates		Parallel to Fuel Plates	
Distance from Reactor Center (in.)	Relative Activity	Distance from Reactor Center (in.)	Relative Activity (Average of Two Runs)
- 0.07	1.000	0.00	0.947
1.69	0.893	2.30	0.962
3.47	0.844	3.50	0.909
4.94	0.745	5.20	0.772
6.87	0.590	6.40	0.668
8.34	0.484	8.10	0.519
9.82	0.384	9.30	0.420
10.11	0.415		

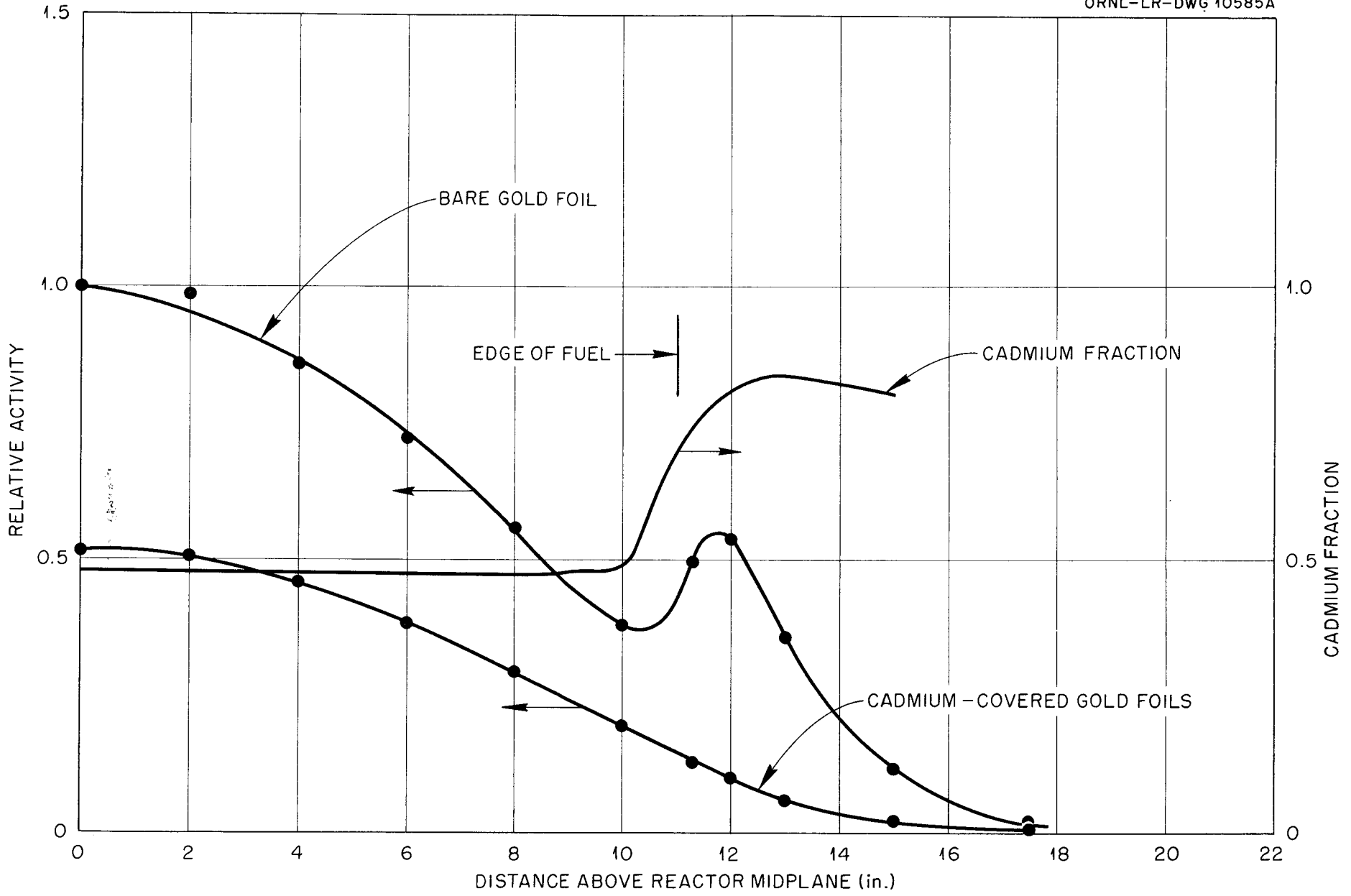


Fig. 20. Vertical Flux Distribution in Element 30 of Reactor with Central APPR Rod Inserted.

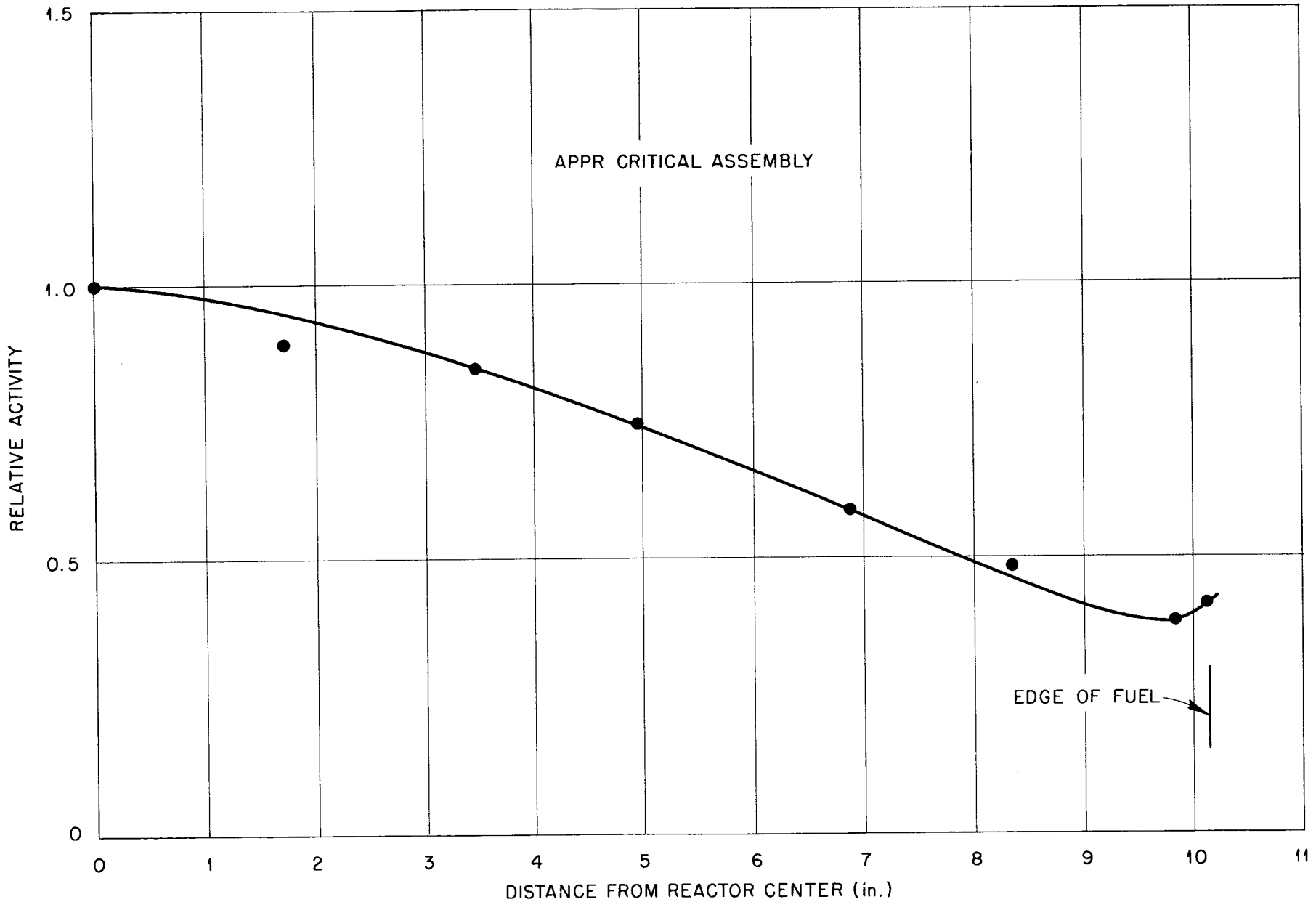


Fig. 21. Horizontal Power Distribution at Midplane in Clean Reactor, Perpendicular to Fuel.

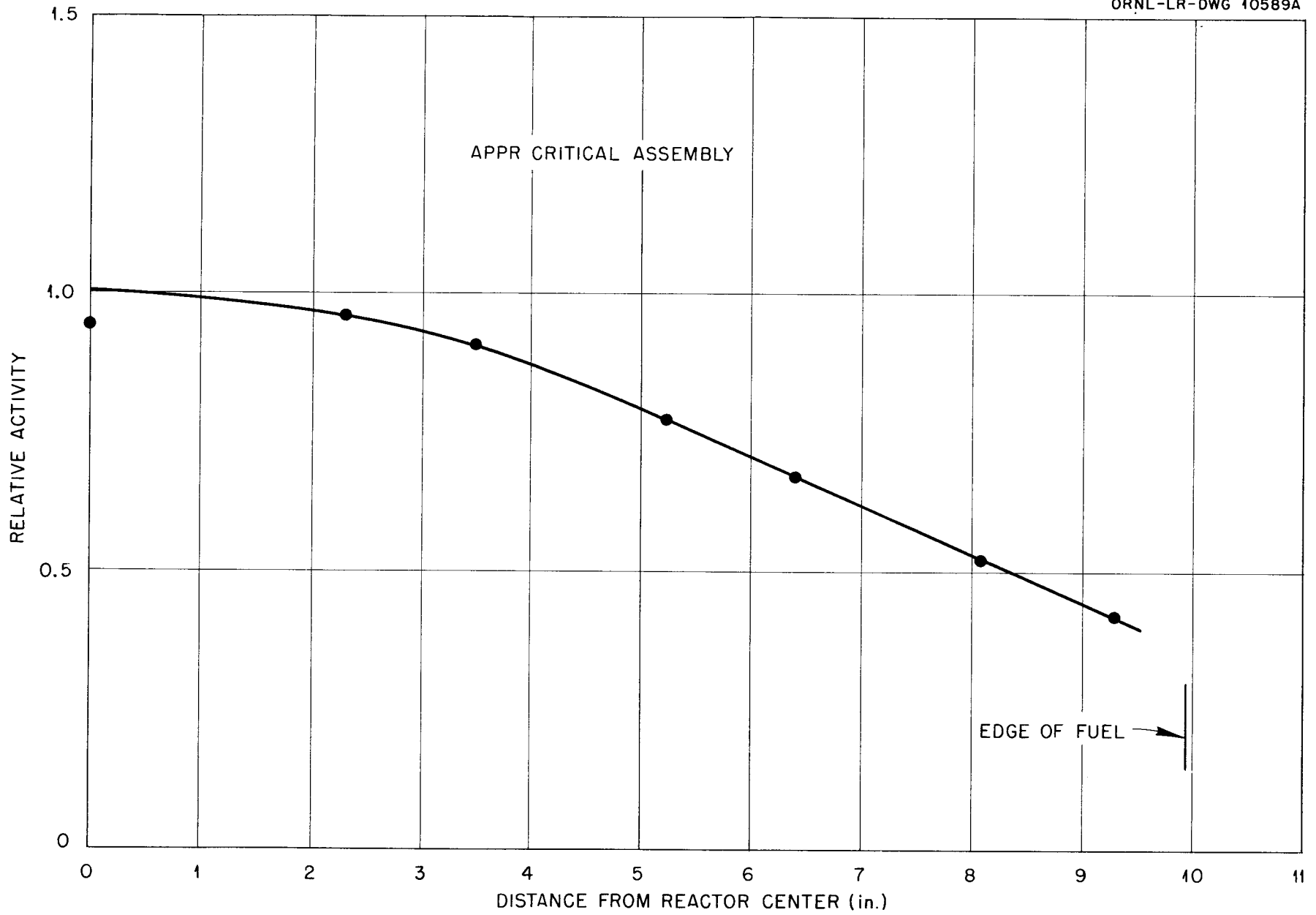


Fig. 22. Horizontal Power Distribution at Midplane in Clean Reactor, Parallel to Fuel.

Table 21. Horizontal Power Distribution in Reactor Containing 255 g of Boron.

Traverse at midplane perpendicular to fuel.

Distance from Reactor Center (in.)	Relative Activity
0.0	1.000
0.66	1.027
2.14	1.026
2.88	0.932
5.09	0.819
5.83	0.718
6.57	0.673
8.78	0.466
9.52	0.444

Table 22. Diagonal Power Distribution in Reactor Containing 255 g of Boron.

Traverse at midplane along diagonal extending from element 23 to 11.

Distance from Reactor Center (in.)	Relative Activity
0.0	1.000
1.06	1.083
3.13	0.944
4.19	0.878
5.25	0.869
7.25	0.680
8.31	0.540
9.34	0.471

Table 23. Horizontal Power Distribution in Clean Reactor with Central APPR Rod Inserted.

Traverse at midplane perpendicular to fuel plates.

Distance from Reactor Center (in.)	Relative Activity
1.69	0.494
2.87	0.941
4.17	1.000
5.18	0.952
6.37	0.880
8.75	0.656
10.13	0.706

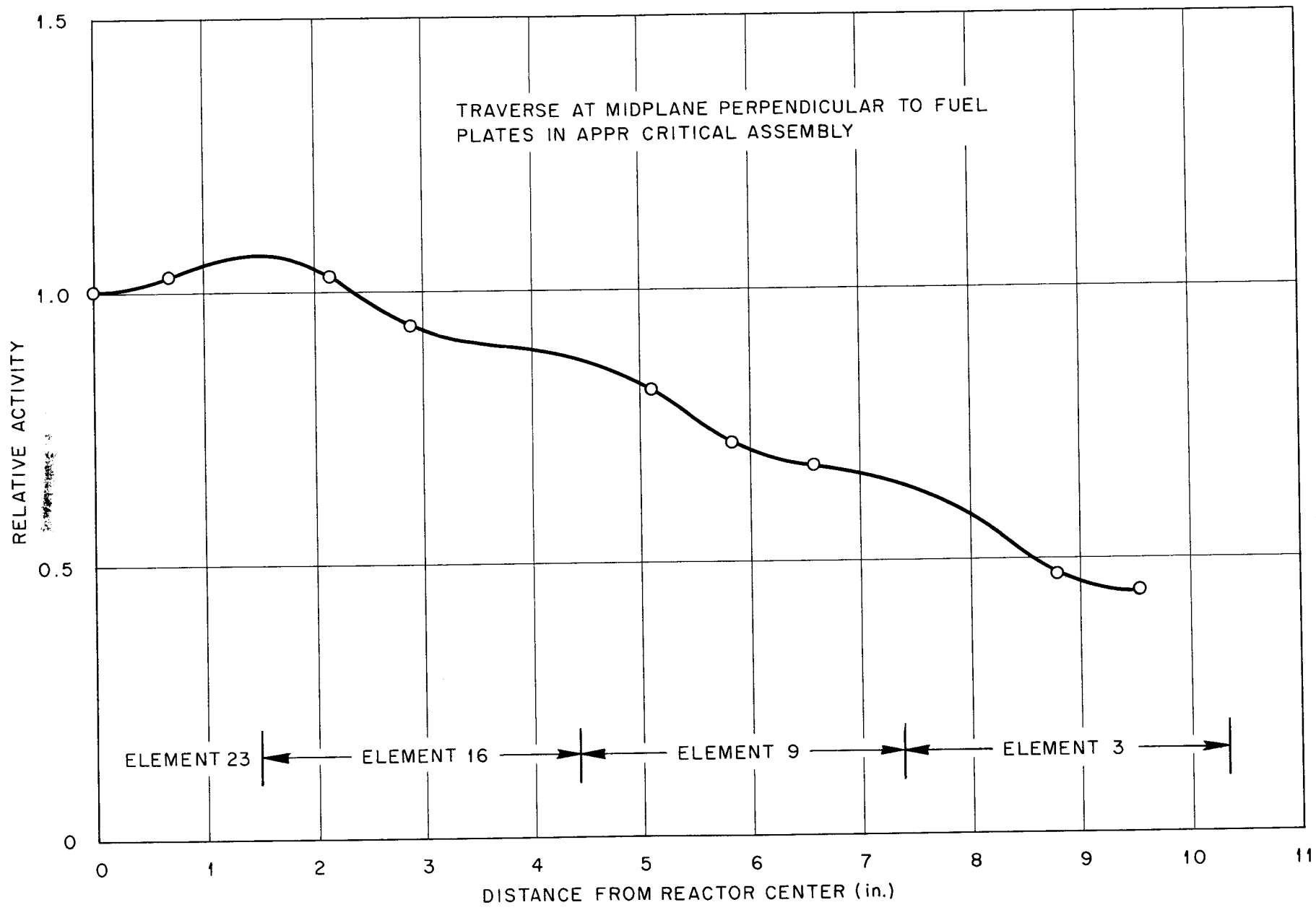


Fig. 23. Horizontal Power Distribution in Reactor Containing 255 g of Boron.

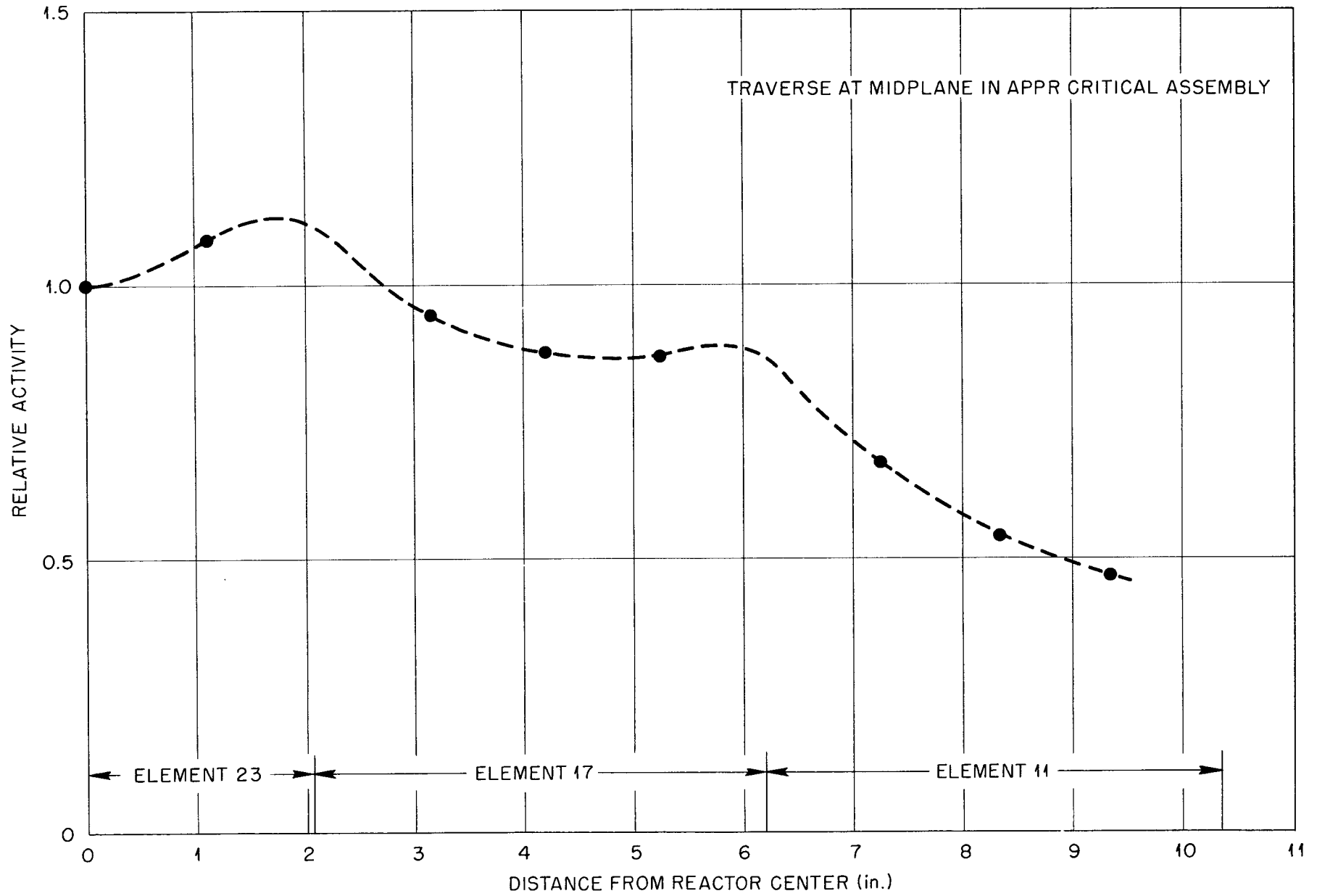


Fig. 24. Diagonal Power Distribution in Reactor Containing 255 g of Boron.

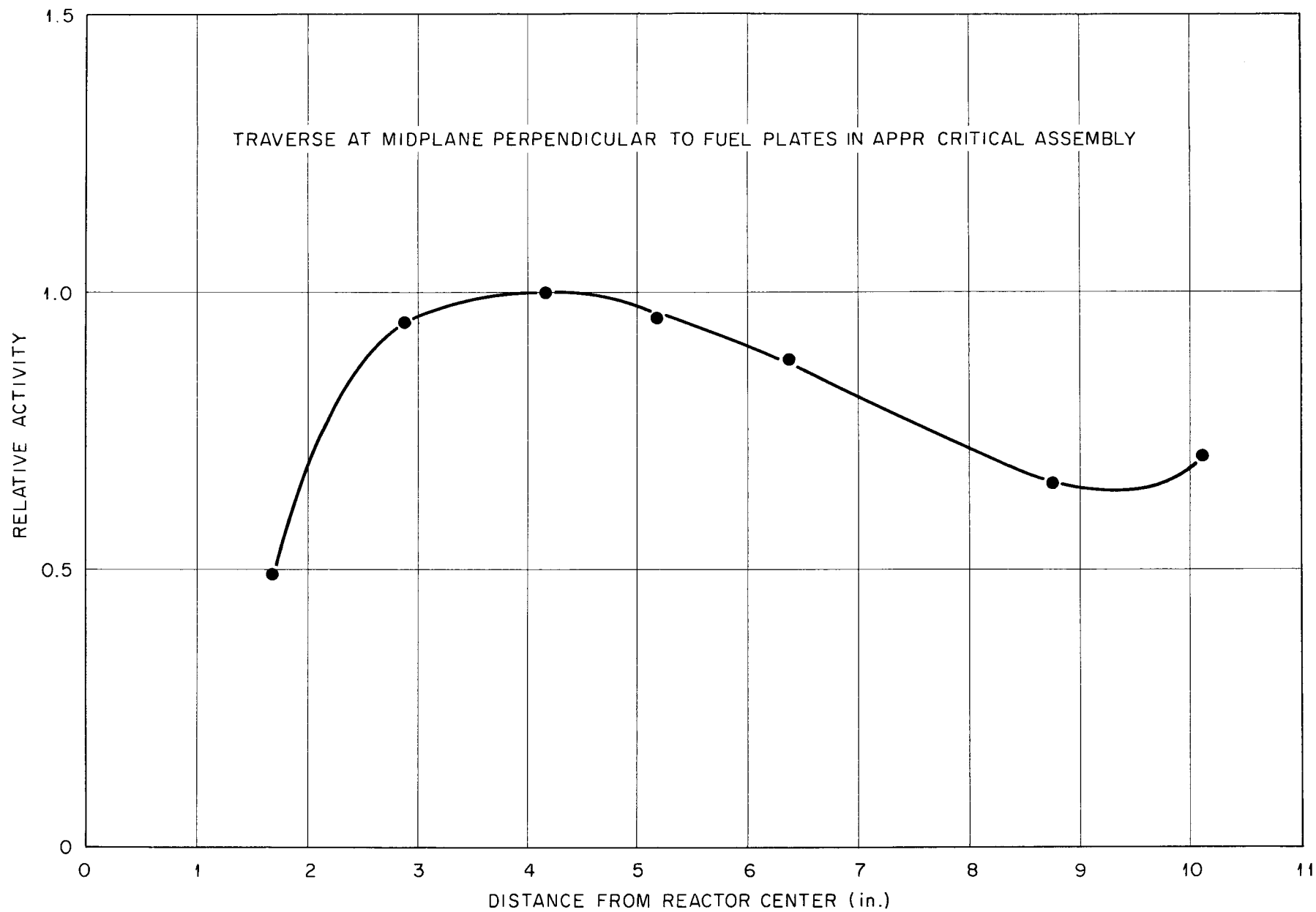


Fig. 25. Horizontal Power Distribution in Clean Reactor with Central APPR Rod Inserted.

Table 24. Horizontal Power Distribution in Clean Reactor with Five APPR Rods Half Inserted.

Traverse parallel to fuel plates.

Distance from Reactor Axis (in.)	Relative Activity		
	13 in. Below Top of Core	17 in. Below Top of Core	21 in. Below Top of Core
0.00	0.806	0.908	0.575
2.90	0.751	0.837	0.537
5.80	0.631	0.691	0.4106
8.70	0.368	0.441	0.273

Table 25. Vertical Power Distribution in Clean Reactor

Distance Above Midplane (in.)	Relative Activity			
	In Element 23		In Element 16	
	Without End Boxes	With End Boxes	With Central APPR Rod Inserted	Average
10.00	0.390	0.386	0.382	0.386
8.00	0.566	0.581	0.553	0.567
6.00	0.730	0.758	0.727	0.738
4.00	0.856	0.873	0.893	0.874
2.00	0.969	0.988	0.955	0.971
0.00	1.000	1.000	1.000	1.000
- 2.00	0.971	0.955		0.963
- 4.00	0.915	0.912	0.877	0.905
- 6.00	0.786	0.814		0.800
- 8.00	0.623	0.632	0.602	0.619
-10.00	0.416	0.424		0.410

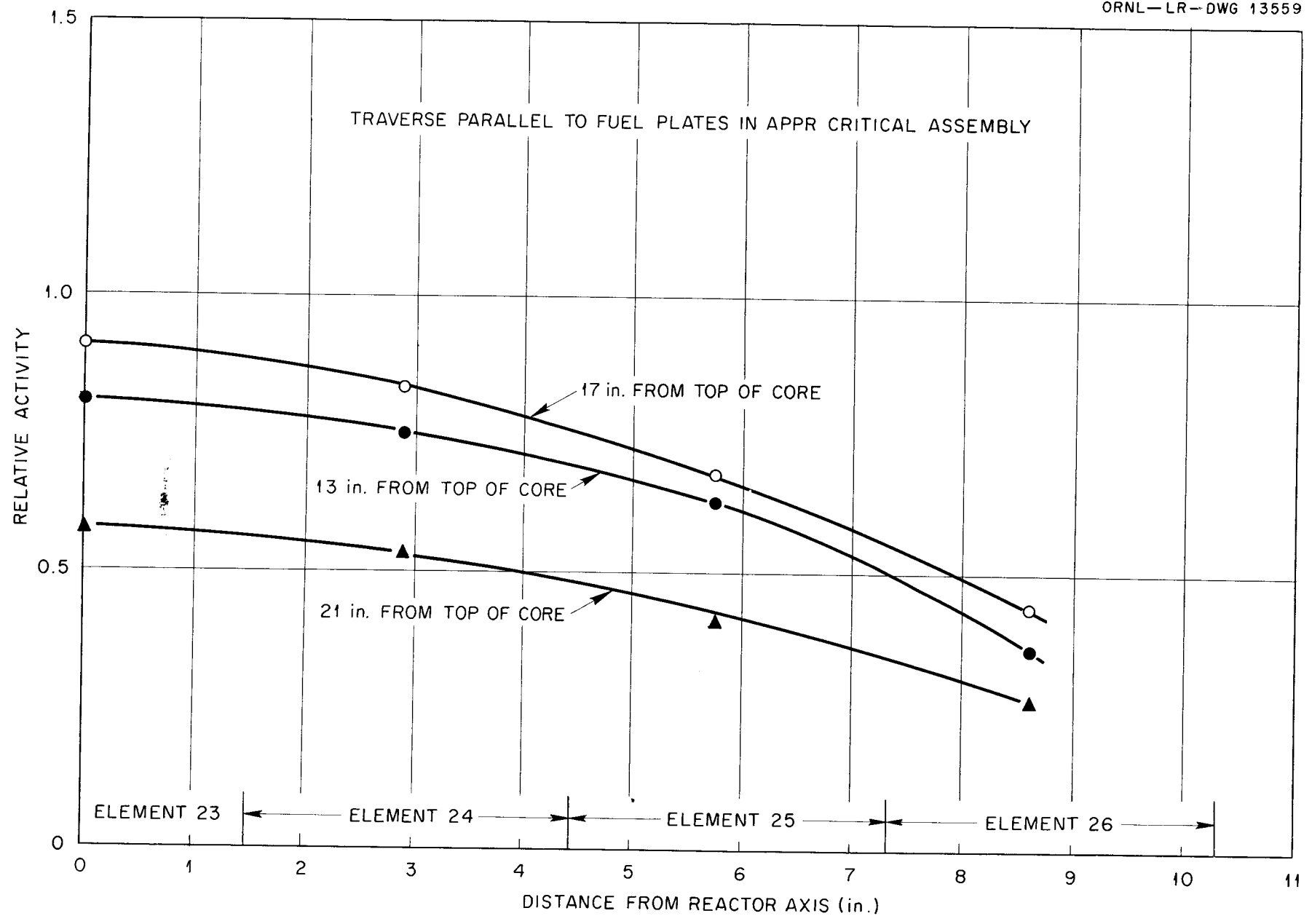


Fig. 26. Horizontal Power Distribution in Clean Reactor with Five APPR Rods Half Inserted .

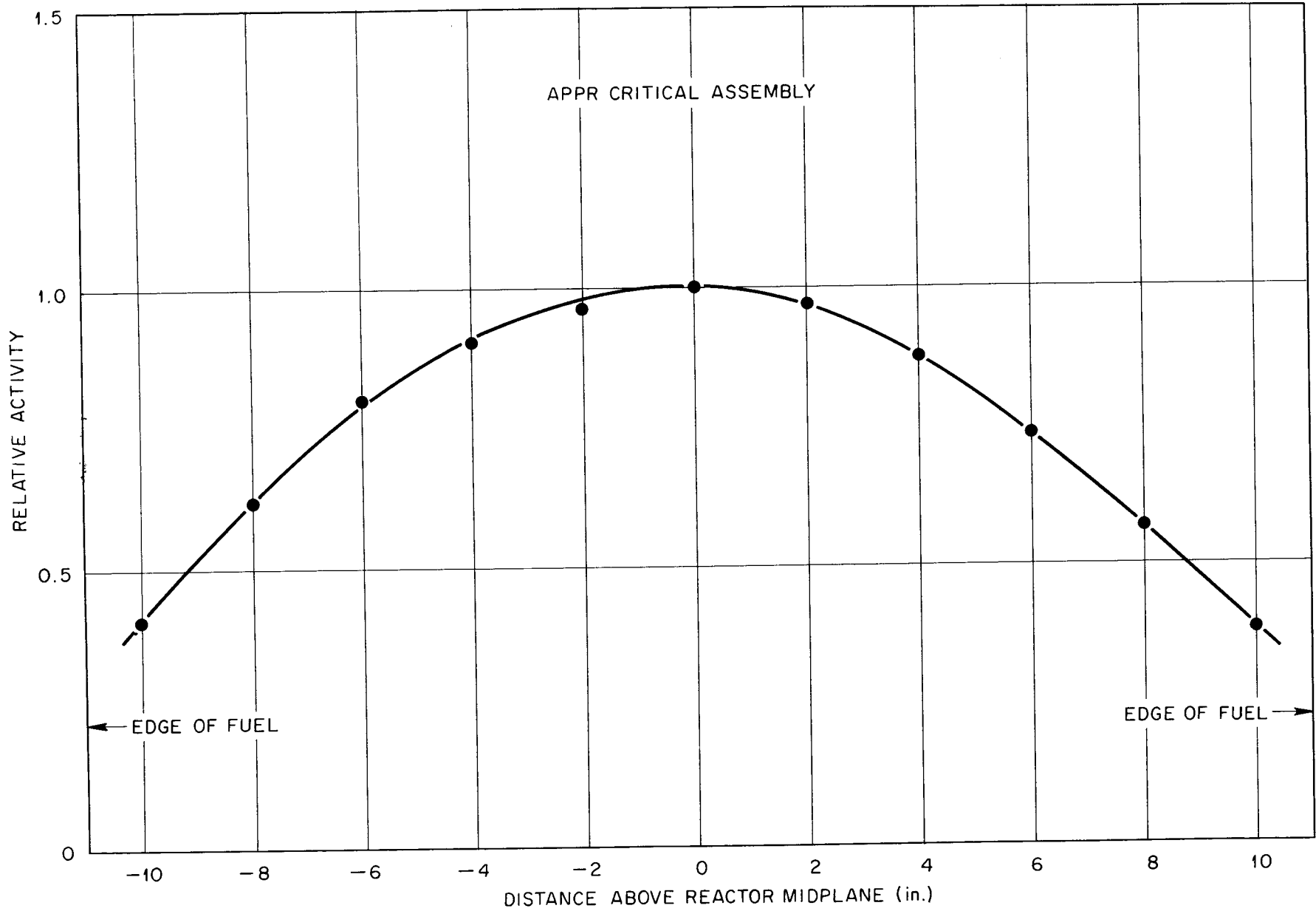


Fig. 27. Vertical Power Distribution in Clean Reactor.

Table 26. Vertical Power Distribution in Element 23 of  
Reactor Containing 255 g of Boron

Distance Above Reactor Midplane (in.)	Relative Activity (Average of Two Runs)
10.00	0.376
8.00	0.567
6.00	0.743
4.00	0.859
2.00	0.968
0.00	1.000
- 2.00	0.945
- 4.00	0.909
- 6.00	0.837
- 8.00	0.710
-10.00	0.469

Table 27. Vertical Power Distribution in Clean Reactor  
with Five APPR Rods Half Inserted

Distance from Top of Reactor Core (in.)	Relative Activity	
	East Side, Slot 1, Element 16	West Side, Slot 18, Element 23
1.00	0.043	
5.00	0.107	
9.00	0.248	
11.00	0.628	
13.00	0.855	0.879
15.00	0.965	0.998
17.00	0.965	1.000
19.00	0.853	0.854
21.00	0.629	0.633
23.00		0.481
25.00		0.187
29.00		0.058
33.00		0.017

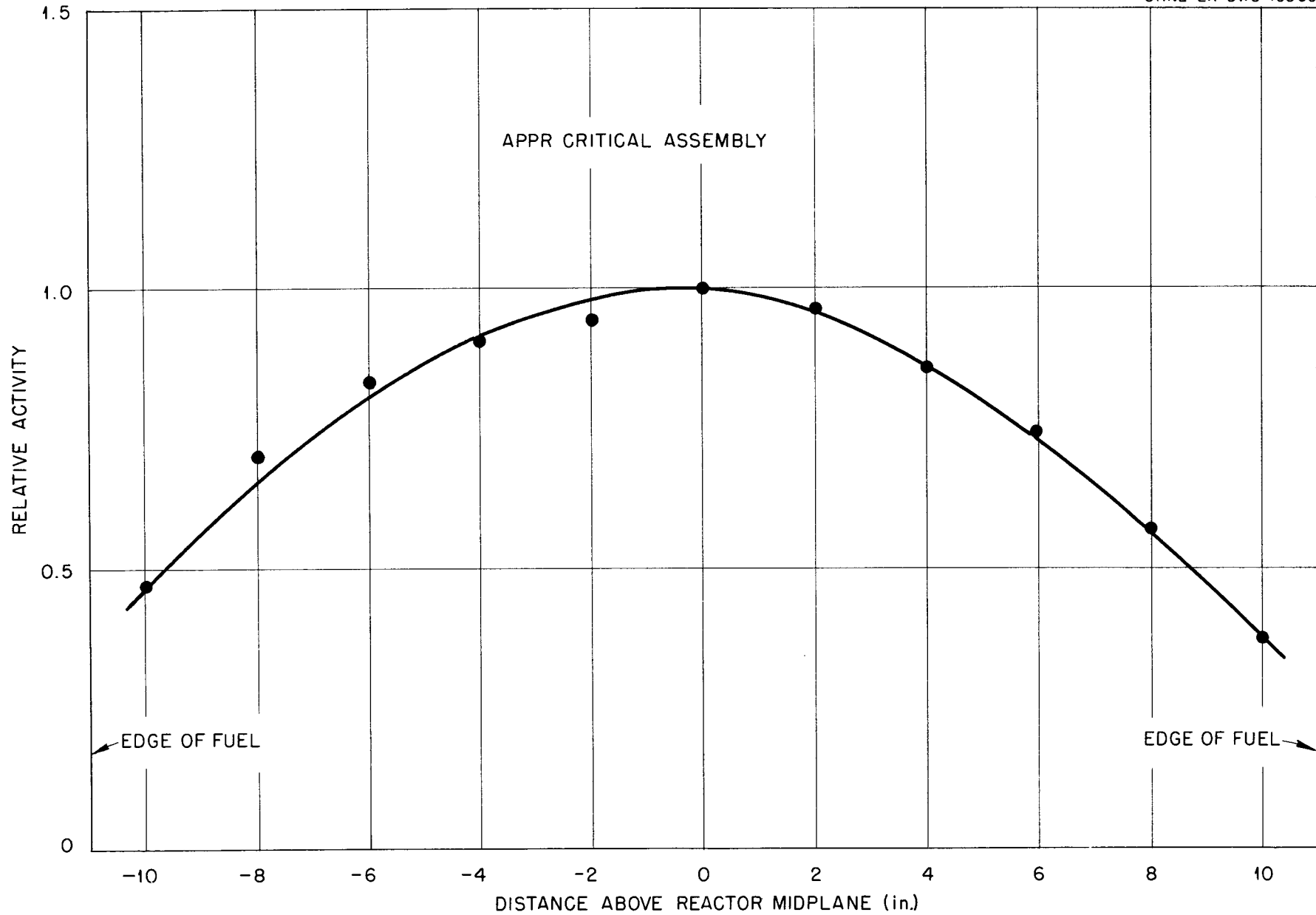


Fig. 28. Vertical Power Distribution in Element 23 of Reactor Containing 255 g of Boron.

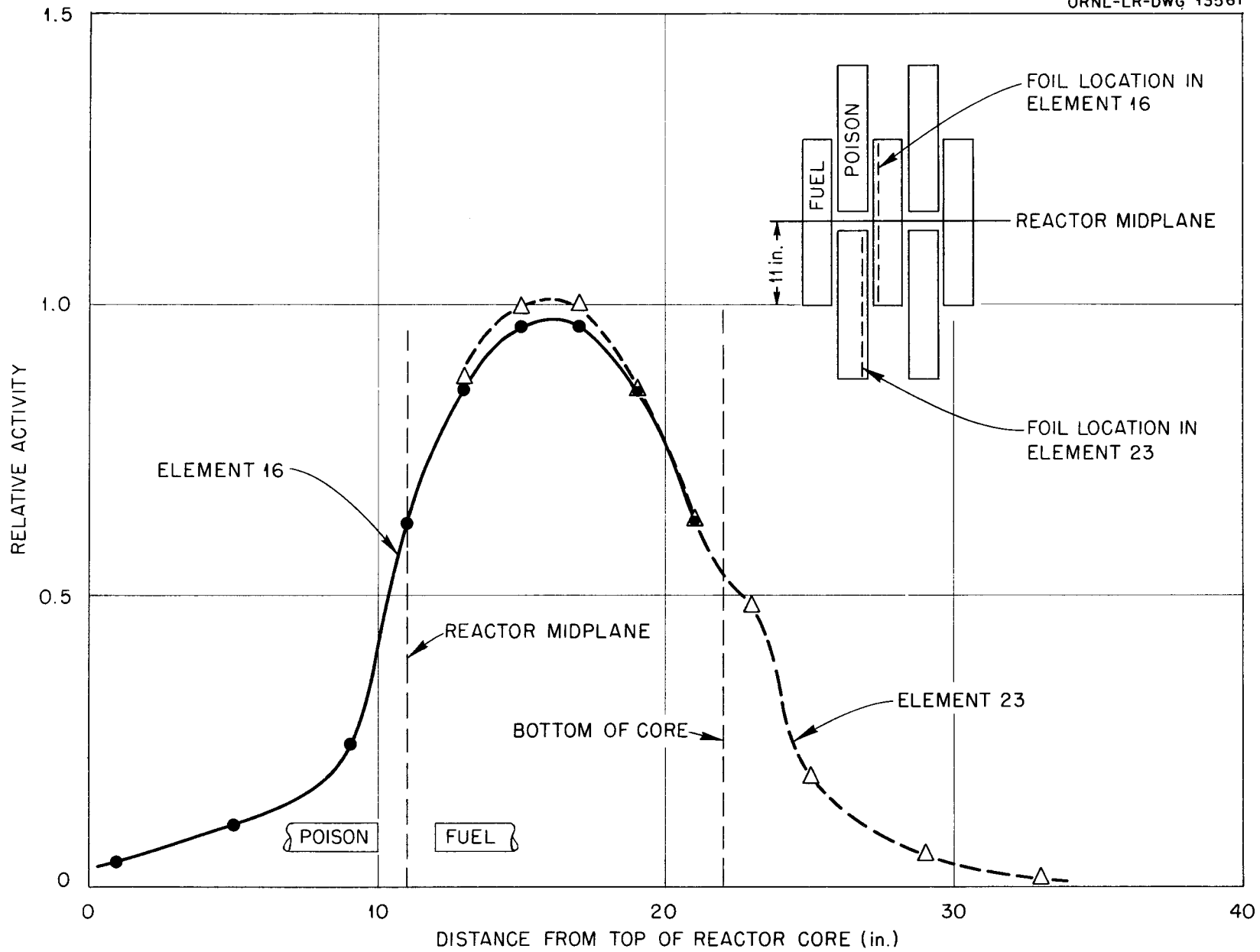


Fig. 29. Vertical Power Distribution in Clean Reactor with Five APPR Rods Half Inserted.

Table 28. Microscopic Flux Traverse in Clean Reactor  
Perpendicular to Fuel.

Traverse at midplane using dysprosium foils.

Element	Location	Slot Side	Relative Activity
23	10	West	4350
23	10	West	4364
23	9	East	4967
23	8	West	4326
23	6	West	4268
23	6	West	4254
23	Midway between 4 and 5		5404
23	3	West	4247
23	2	West	4673
23	1	West	4009
23	SS Side	East	4909
16	18	West	4190
16	17	West	4693
16	16	West	4349
16	Midway between 14 and 15		5320
16	13	West	4504
16	13	East	4428
16	Midway between 11 and 12		5163
16	10	West	4099
16	10	West	4137
16	9	West	4377

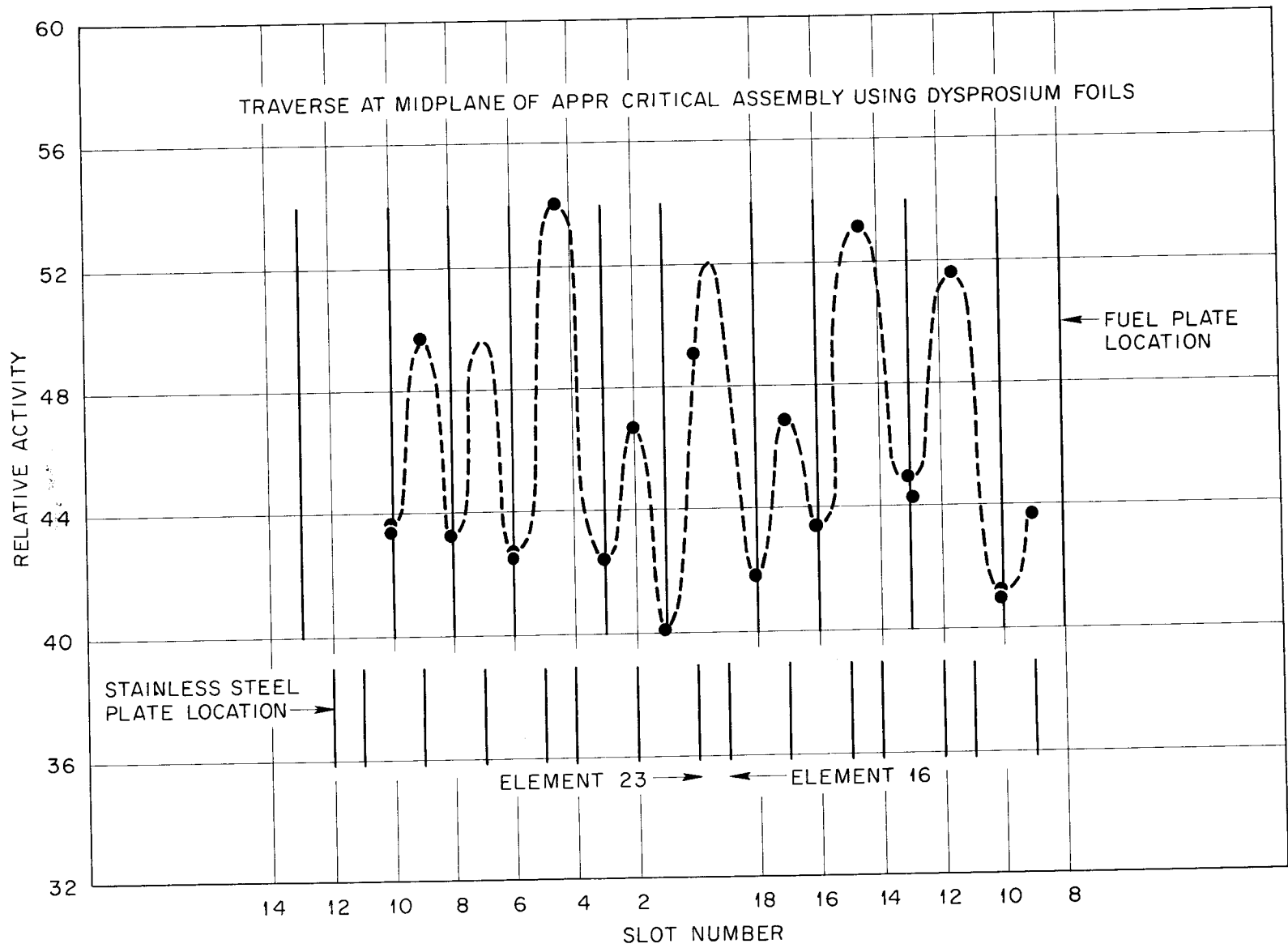


Fig. 30. Microscopic Flux Traverse in Clean Reactor, Perpendicular to Fuel.

Table 29. Microscopic Flux Traverse in Clean Reactor with APPR Element in Position 23.

Traverse perpendicular to fuel plates using dysprosium foils.

Element	Location		Relative Activity
	Slot	Slot Side	
23	11	East	4892
23	9	East	4807
23	Midway between 8 and 9		5138
23	Midway between 7 and 8		5175
23	7	West	4864
23	6	West	4645
23	5	East	4655
23	Midway between 4 and 5		5105
23	3	West	4812
23	3	East	4779
23	2	East	4893
23	1	East	4743
16	SS Side		4986
16	18	East	4249
16	17	West	4685
16	16	East	4320
16	15	West	5048
16	13	East	4614
16	13	East	4506
16	10	East	4211
16	10	East	4060

Table 30. Microscopic Flux Traverse in Clean Reactor Parallel to Fuel.

Traverse at midplane using dysprosium foils.

Distance from Edge of Element 23 (in.)	Relative Activity	
	With Normal Element in Position 23	With APPR Element in Position 23
1.40	4350	4892
1.40	4364	
2.05		4910
2.30	4807	
2.42		5078
2.81	5609	5423
3.28		4750
3.40	4621	
4.30	4059	4081
5.20	4264	

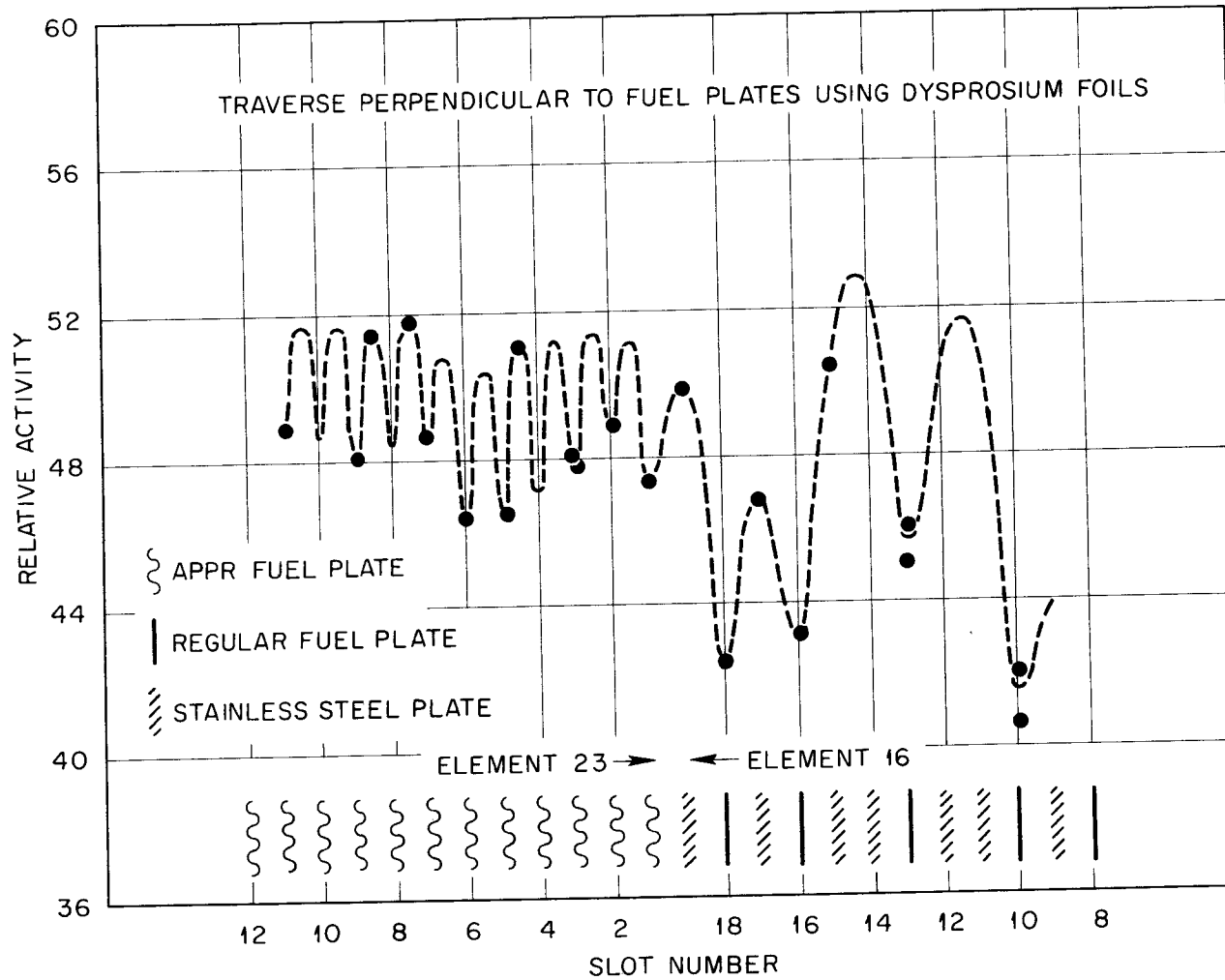


Fig. 31. Microscopic Flux Traverse in Clean Reactor with APPR Element in Position 23.

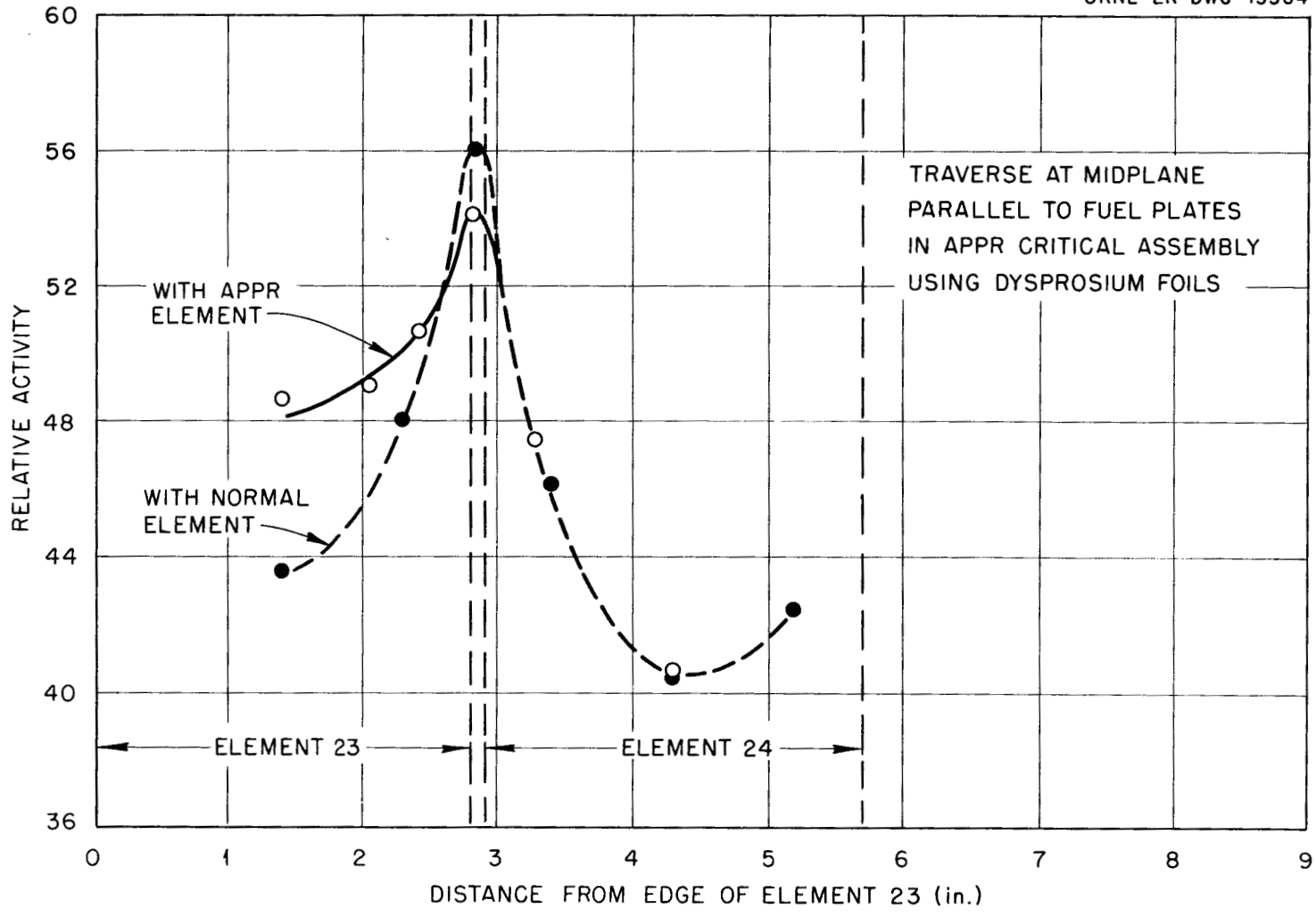


Fig. 32. Microscopic Flux Traverse in Clean Reactor Parallel to Fuel.

Table 31. Microscopic Flux Traverse in Reactor Containing  
255 g Boron.

Traverse at midplant perpendicular to fuel plates  
using dysprosium

Element	Location		Relative Activity
	Slot	Slot Side	
23	10	West	1500
23	9	West	1446
23	8	West	1551
23	8	West	1544
23	7	West	1521
23	6	West	1543
23	Between 5 and 6		1688
23	5	West	1451
23	4	West	1412
23	4	West	1426
23	3	West	1650
23	Between 2 and 3		1841
23	1	West	2094
23	SS Side	East	2505
16	SS Side	West	2578
16	18	West	2120
16	17	West	1860
16	17	West	1869
16	Between 15 and 16		1804
16	15	West	1640
16	14	West	1427
16	14	West	1369
16	13	West	1478
16	12	West	1450
16	11	West	1411
16	9	West	1279

Table 32. Flux Distribution at Perimeter of Element 23 in  
Reactor Containing 255 g of Boron.

Traverse in horizontal midplane using dysprosium foils.

Location <sup>a</sup> (deg)	Relative Activity
0	25.05
40	29.88
90	24.38
130	25.70
180	24.00

a. Radius toward element 16 taken as 0 deg.

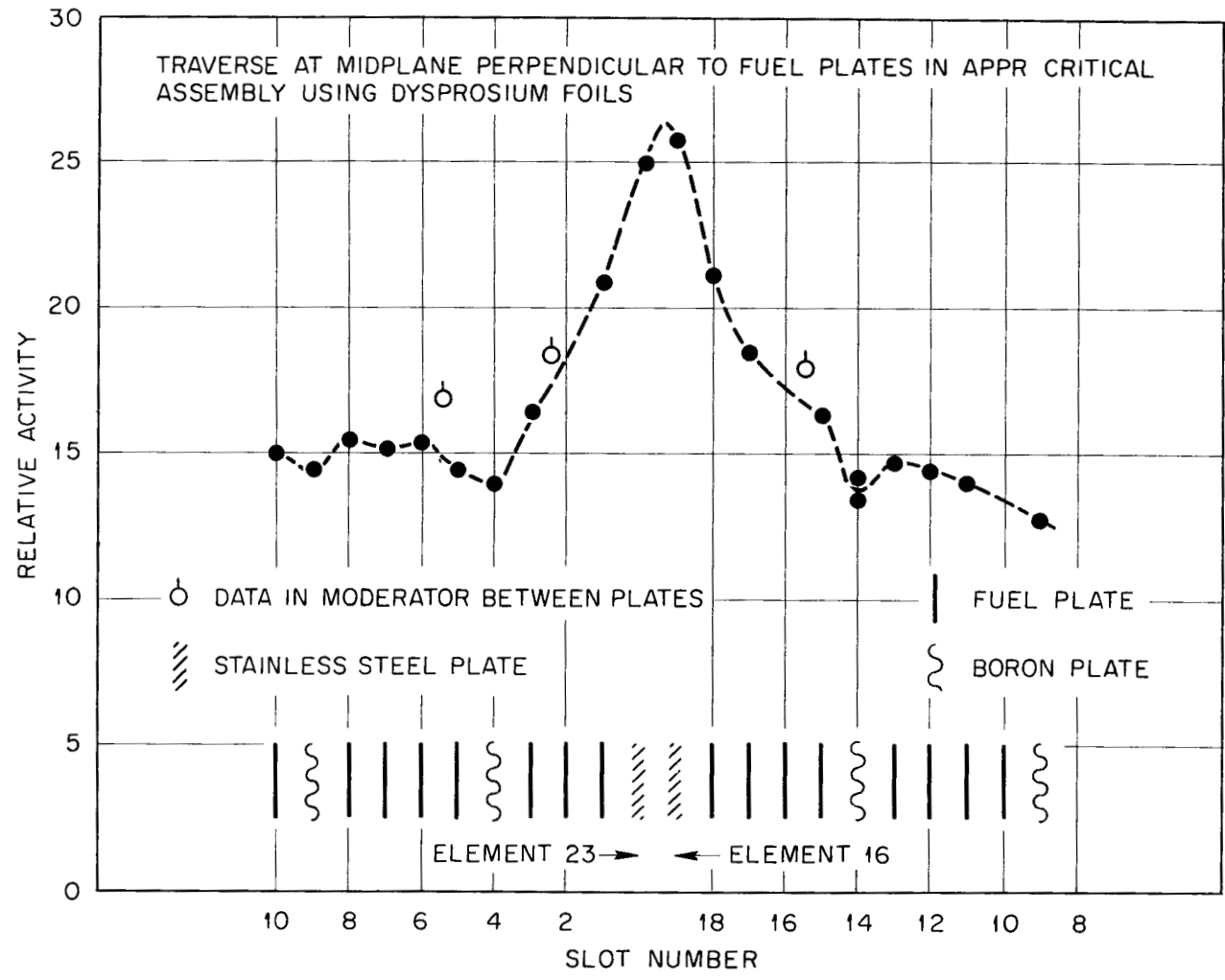


Fig. 33. Microscopic Flux Traverse in Reactor Containing 255 g of Boron.

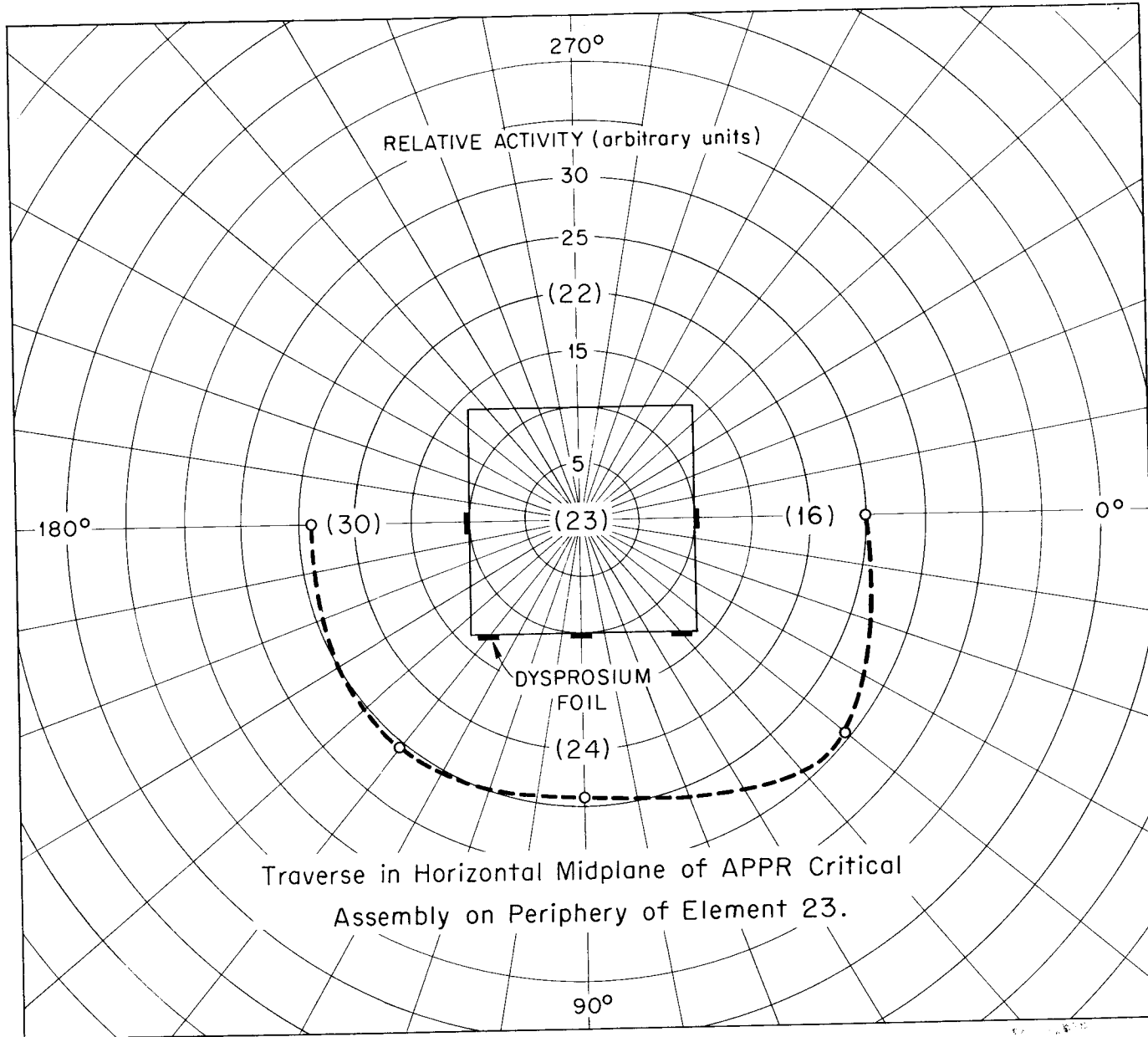


Fig. 34. Flux Distribution at Perimeter of Element 23 in Reactor Containing 255 g of Boron.

Table 33. Power Distribution at Corner of Clean Reactor.

Traverse in horizontal midplane using 0.500 in. diameter aluminum catcher foils.

Perpendicular to Fuel			
Element	Location		Relative Activity (Normalized to 1.0 at Reactor Center)
	Slot	Distance from N-S $\xi$ (in.)	
11	1	7.16	0.401
5	18	7.60	0.389
5	16	7.89	0.388
5	10	8.78	0.355
5	3	9.82	0.285
5	1	10.11	0.316

Parallel to Fuel			
Element	Location		Relative Activity (Normalized to 1.0 at Reactor Center)
	Slot	Distance from E-W $\xi$ (in.)	
11	1	6.83	0.401
12	1	7.95	0.414
12	1	8.55	0.387
12	1	9.14	0.339
12	1	9.74	0.325

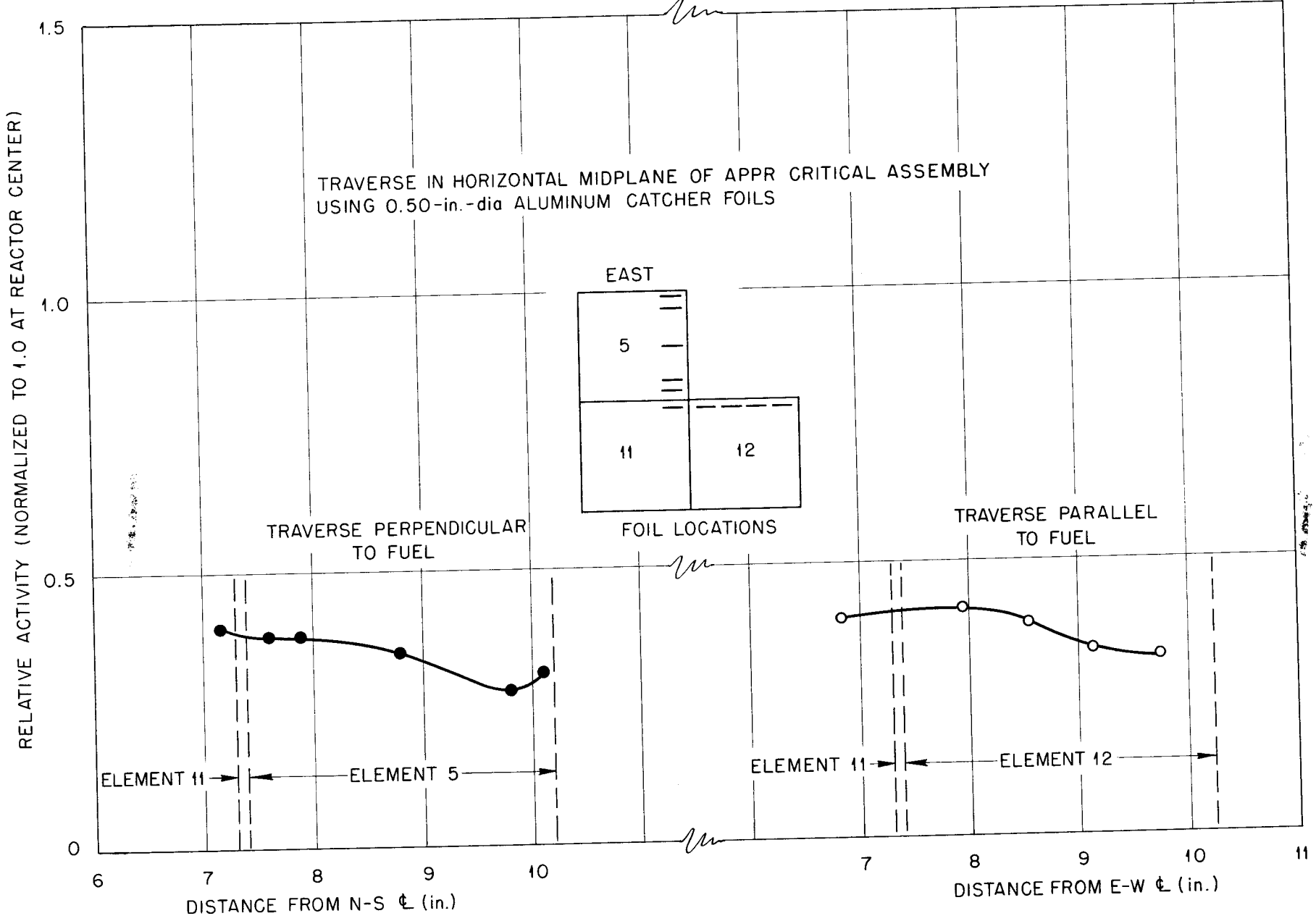


Fig. 35. Power Distributions at Corner of Clean Reactor.

Appendix A

DETAILED COMPONENT SPECIFICATIONS

Dimensional and material specifications of the fuel boxes, fuel plates, boron plates, and steel plates are given below.

Fuel Box Specifications<sup>4</sup>

Design Data

Over-all dimensional specifications	Box type I, ORNL Dwg. D-2-02-015-38 <sup>4</sup>
Side plate dimensions, in.	2.786 x 31 x 0.078
Slot dimensions in side plate, in.	0.056 wide x 0.050 deep on 0.148 centers
Number of slots in side plate	18
End plate dimensions, in.	2.800 x 31 x 0.031
Cross-sectional metal area in box, in. <sup>2</sup>	0.5088
Cross-sectional metal area in 18 plates (fuel, boron, or steel plates), in. <sup>2</sup>	1.2254
Area of cell, in. <sup>2</sup>	8.5608
Volume fraction of metal in cell	0.2026

Material Specifications

Side and end plates	Wrought stainless steel type 304L or 304 commercial sheet
---------------------	---

Method of Material Identification

Side and end plates	Chemical analysis
---------------------	-------------------

Fuel Plate Specifications<sup>4</sup>

Design Data

Over-all dimensional specifications	Test plate types D, E, F, and G, ORNL Dwg. No. D-2-02-015-37 <sup>4</sup>
Dimensions of uranium foils, in.	
Full foils	2.500 x 22 x 0.002
Half foils	1.250 x 22 x 0.002
Mass of uranium foils, g	
Full foils	33.4 ± 0.20
Half foils	16.7 ± 0.10
Outside dimensions of stainless steel cladding (thickness at $\phi$ ), in.	2.723 x 23 x 0.024
Clad-core-clad thickness, mil	11.1-2-11.1

Material Specifications

Uranium foil	U-235 enrichment 93.2%
Stainless steel cladding	Wrought stainless steel type 304 commercial sheet
Adhesive	Type EC-776 adhesive Minnesota Mining and Manufacturing Company

Method of Material Identification

Uranium	Mass spectrographic analysis
Stainless steel	Spectrographic analysis
Adhesive	Chemical analysis

Boron Plate Specifications<sup>5</sup>

Design Data

Over-all dimensional specifications	Test plate types B and C	
Core dimensions (nominal), in.	ORNL Dwg. No. C-2-02-015-36 <sup>5</sup>	
Outside dimensions (nominal), in.	2.5 x 22 x 0.015	
Clad-core-clad thickness, mil	2.723 x 23 x 0.025	
Type of plate	5-15-5	
Number of plates	B	C
Natural boron content per plate, g	190	50
	1.889 +0.000	0.944 +0.000
	-0.004	-0.002
Core mixture composition, wt%	2.33 B <sub>4</sub> C	1.67 B <sub>4</sub> C
(based on B <sub>4</sub> C with 78.3% B)	97.67 SS	98.33 SS
B <sub>4</sub> C content per plate, g	2.411	1.206
(based on B <sub>4</sub> C with 78.3% B)		
Stainless steel content per plate, g	198.28	202.16

Material Specifications

Core material	Stainless steel type 304 (-100)
Prealloyed steel powder	mesh size, and irregular particle shape
Boron carbide powder	Ground and screened to (-325) mesh size
Frame material	Wrought stainless steel type 304L or 304 commercial sheet
Cover material	Wrought stainless steel type 304L or 304 commercial sheet

Method of Material Identification

B <sub>4</sub> C	Chemical analysis
Prealloyed steel powder	Chemical analysis

~~CONFIDENTIAL~~

Frame and clad stainless steel

Chemical analysis

Inspection

Chemical analysis of the boron content and distribution in one plate out of each blending batch. A further check on the distribution was made by a radiographic method which was necessary to locate the core for trimming the plate to size.

Steel Plate Specifications

Design Data

Over-all dimensional specifications

Plate type A, ORNL Dwg.

Outside dimensions (nominal), in.

No. C-2-02-015-34

Number of plates

2.723 x 23 x 0.025

Weight of plates, g

700

206.03

Material Specifications

Plate material

Wrought stainless steel  
type 304L or 304 commercial  
plate

Method of Material Identification

Plate material

Chemical analysis

~~CONFIDENTIAL~~

~~CONFIDENTIAL~~

Appendix B

SPECTROGRAPHIC ANALYSES OF TYPE 304 STAINLESS STEEL SAMPLES

Samples of type 304 stainless steel from a fuel box, a fuel plate, and a steel plate were spectrographically analyzed as follows:

<u>Sample</u>	<u>Element</u>	<u>Analyses (at.%)</u>
Fuel box	Cr	16.4
	Ni	8.9
	Mn	0.5
	Si	1.
	B	< 0.0006
	Cd	< 0.0005
	Gd	< 0.0001
	Fuel plate sample I	Cr
Ni		8.3
Mo		0.3
Mn		1.1
Si		0.6
B		< 0.0006
Cd		< 0.0005
Cb		< 0.1
Al		< 0.05
Be		< 0.001
Co		0.5
Cu		1
Ti		0.02
V		0.05
Fuel plate sample II		Cr
	Ni	8.0
	Mo	0.3
	Mn	1.2
	Si	0.6
	B	< 0.0006
	Cd	< 0.0005
	Cb	< 0.1
	Al	< 0.05
	Be	< 0.001
	Co	0.5
	Cu	1
	Ti	0.02
	V	0.05

~~CONFIDENTIAL~~

~~CONFIDENTIAL~~

<u>Sample</u>	<u>Element</u>	<u>Analyses (at %)</u>
Fuel plate* sample III	Cr	15.4
	Ni	14.7
	Mo	0.2
	Mn	0.7
	Si	0.5
	B	< 0.0005
	Cd	< 0.0005
	La	< 0.5**
	Ce	< 120**
	Gd	< 0.5**
Fuel plate* sample IV	Cr	20
	Ni	11
	Mo	0.15
	Si	0.35
Steel plate	Cr	17.1
	Ni	8.6
	Mo	0.4
	Mn	0.8
	Si	0.7
	B	< 0.0006
	Cd	< 0.0005
	Gd	< 0.001

\* The steel used in the 100 fuel plates fabricated in Oak Ridge used steel represented by samples III and IV.

\*\* Concentrations of these rare earth impurities are expressed as parts per million of the rare earth oxide, Re<sub>2</sub>O<sub>3</sub>.

~~CONFIDENTIAL~~

Appendix C

FUEL PLATE FABRICATION

The fuel plates for the APPR critical experiment consisted of a glued sandwich of stainless steel which encased the uranium foil.<sup>4</sup> One steel plate was larger, and the overlap was folded over to seal the edges. The uranium foils were rolled to a thickness of approximately 0.002 in. and cut to size. Overweight foils were brought to mass specifications by electrolytic etching. Foils and stainless steel were cleaned with acetone, coated with an adhesive (Minnesota Mining and Manufacturing Company EC-776), and allowed to dry. Final assembly was accomplished by bending the edges and stamping in a press for closure. Dimensional tolerances on the length and width were maintained by performing the stamping operation inside a die.

A severe bulging of a large fraction of the plates was observed when the finished uranium plates were received from the fabricator. Since the plate distension increased with time, some of the edges of the plates pulled apart and vented the gas pressure. Some plates eventually became 0.8 in. thick whereas the over-all thickness of the stainless steel, uranium foil and adhesive was less than 0.025 in. It was also noted that many of the plates were not adequately sealed as they bubbled when immersed in water.

Examination of some of the first plates showed excess solvent, and the adhesive was tacky and did not adhere adequately to either the steel or uranium. Although this solvent problem was eliminated by longer drying of the adhesive before assembly and by heat curing after assembly the plates continued to bulge.

Fluoroscopic examination of some of the plates after about six weeks use showed that some uranium foils were badly corroded, probably the result of water leaking into them during the critical experiment. It became apparent that some of the plates which were not distended were those from which gas could escape. On several occasions the gas was vented from groups of bulging plates and then they were resealed.

The largest void volume measured, but probably not the largest void volume that existed, was 4363 cc for 360 plates. This excess volume averages 12.1 cc per plate or a 46.7% increase over the plate volume of 26 cc. By opening and venting the gas in the most distended plates, approximately one-third of the total, the void volume was reduced to half of its previous value.

The primary cause of the bulging of the plates is believed to be hydrogen gas formation from a uranium-water reaction. The source of water in these plates was probably adsorbed moisture on the uranium and steel and possibly small amounts of water in the adhesive. The final 110 plates prepared for the experiment were assembled at Oak Ridge using utmost care to eliminate moisture. The uranium foils were stored in desiccators with Drierite. The stainless steel plates were cleaned and stored in a dry box.

The foils and steel were coated in a dry box with Dow A-4000 silicon adhesive, and after complete drying, the uranium foil was placed between the stainless steel plates. These plates were pressed by a total force of 40 tons in a hydraulic press prior to final assembly. Extra adhesive was used on the edges prior to final closure to insure that the edges did not leak. Final closure in the die and punch press as well as the hydraulic press operation had to be accomplished out of the dry box. None of the plates bubbled when immersed in water, and although the number of bulging plates was greatly reduced, the problem was not completely eliminated.

Appendix D

TYPICAL PLATE ARRANGEMENTS WITHIN A FUEL ELEMENT

The typical plate arrangements for various critical assembly experiments are given below in Table D-1. These loadings were chosen to distribute the uranium as uniformly as possible, cognizant of the fact that the end plates of the fuel element box were two extra stainless steel plates.

Table D-1. Typical Plate Arrangements Within a Fuel Element

Key: F = Full fuel plate                      S = Stainless steel plate  
      F/2 = Half fuel plate                    B = Boron plate

Slot Number	Clean Critical	One Boron Plate per Box	Two Boron Plates per Box	Three Boron Plates per Box
1	F	F	F	F
2	S	S	F <sup>b</sup>	F
3	F	F	F	F
4	S	S	B	B
5	S	F	F	F
6	F	F	F	F
7	S	S	S	F/2
8	F/2	F/2 <sup>a</sup>	F	F
9	S	S	S	B
10	F	F	F	F
11	S	F	F	F
12	S	S	S	F <sup>c</sup>
13	F	F	F	F
14	S	B	B	B
15	S	S	S	F
16	F	F	F	F
17	S	S	F	F
18	F	F	F	F
Total mass of U-235 (kg)	10.496	13.326	16.701	20.106
Total mass of Boron (g)	0.0	85.0	170.0	255.0

- a. Slot 8 of boxes 7 and 35 contained full fuel plates.
- b. Slot 2 of boxes 7, 11, 35 and 39 contained half fuel plates.
- c. Slot 12 of boxes 8, 10, 21, 36 and 38 contained steel plates.

Appendix E

CALCULATION OF METAL VOLUME PERCENT IN CORE

The volume percent of each material in the core was determined from the area percent of the material in a fuel element taken as a unit cell. These components were the fuel box, steel plates, uranium plates, and boron plates with the remaining volume filled with water. The volume percent of boron at any time was negligible compared with the volumes of other materials. When possible, average measured dimensions were used to find component areas rather than those specified for the experiment. In some cases there was a considerable difference between the design and the measured average dimensions, although all components met design tolerances.<sup>17</sup> Component areas were calculated at the horizontal midplane of the core.

1. Area of steel in a fuel box:	
Two end plates, 2.816 x 0.0305 in.	0.1718 in. <sup>2</sup>
Two side plates (2.786 x 0.075 in.) - 18 (0.050 x 0.056 in.)	0.3172 in. <sup>2</sup>
Total	<u>0.489 in.<sup>2</sup></u>
2. Area of steel in a steel plate: 0.025 x 2.723 in.	0.0681 in. <sup>2</sup>
3. Area of steel in full and half fuel plates: (2.723 + 2.638 + 2 x 0.125) x 0.0106 in.	0.0595 in. <sup>2</sup>
4. Area of steel in a boron plate: 2.723 x 0.025 in.	0.0681 in. <sup>2</sup>
5. Area of uranium:	
Full fuel plate 2.5 x 0.002 in.	0.005 in. <sup>2</sup>
Half fuel plate 1.25 x 0.002 in.	0.0025 in. <sup>2</sup>
6. Area of a unit cell: 2.900 x 2.952 in.	8.5608 in. <sup>2</sup>

The calculation of metal volume percent in the cold clean critical configuration is given below. The element loading was as follows:

- 7 full fuel plates per element
- 1 half fuel plate per element
- 10 steel plates per element
- 0 boron plates per element.

The component areas in a unit cell are as follows:

Steel in the fuel box	0.489 in. <sup>2</sup>
Steel in steel plates, 10 x 0.0681 in. <sup>2</sup>	0.681 in. <sup>2</sup>
Steel in fuel plates, 8 x 0.0595 in. <sup>2</sup>	0.476 in. <sup>2</sup>
Uranium in fuel plates, 7-1/2 x 0.005 in. <sup>2</sup>	0.0375 in. <sup>2</sup>
Total metal area	1.684 in. <sup>2</sup>

The metal volume percent is:

$$\frac{1.684 \times 100\%}{8.5608} = 19.67\%$$